Stochastic quantum trajectories demonstrate the Quantum Zeno Effect in an open spin system

Sophia M. Walls, Julien M. Schachter, Haocheng Qian and Ian J. Ford Department of Physics and Astronomy, University College London, Gower Street, London, WC1E 6BT, United Kingdom

We investigate the Quantum Zeno Effect in spin 1/2, spin 1 and spin 3/2 open quantum systems undergoing Rabi oscillations. The systems interact with an environment designed to perform continuous measurements of an observable, driving the systems stochastically towards one of the eigenstates of the corresponding operator. The system-environment coupling constant represents the strength of the measurement. Stochastic quantum trajectories are generated by unravelling a Markovian Lindblad master equation using the quantum state diffusion formalism. This is regarded as a better representation of system behaviour than consideration of the averaged evolution since the latter can mask the effect of measurement. Complete positivity is maintained and thus the trajectories can be considered as physically meaningful. Increasing the measurement strength leads to greater dwell by the system in the vicinity of the eigenstates of the measured observable and lengthens the time taken by the system to return to that eigenstate, thus demonstrating the Quantum Zeno Effect. For very strong measurement, the Rabi oscillations develop into randomly occurring near-instantaneous jumps between eigenstates. The stochastic measurement dynamics compete with the intrinsic, deterministic quantum dynamics of the system, each attempting to drive the system in the Hilbert space in different ways. As such, the trajectories followed by the quantum system are heavily dependent on the measurement strength which other than slowing down and adding noise to the Rabi oscillations, changes the paths taken in spin phase space from a circular precession into elaborate figures-of-eight.

I. INTRODUCTION

The Quantum Zeno Effect (QZE), also known as the Turing Paradox, is the suppression of the unitary time evolution of a system brought about by repeated measurements. The first general derivation of the QZE was performed by Degasperis et al. in 1974 [1] but the effect was formally characterised by Misra and Sudarshan [2], who showed in 1977 that the probability that a system should remain in an initial state will approach unity as the frequency of projective measurements made on it tends to infinity. The QZE was named after the Greek philosopher Zeno's paradox, which suggested that if an arrow were continuously observed, it would (arguably) appear to be motionless and thus would never reach its target. Any disturbance in the rate of change of a quantum system as a result of measurement can be considered to be a demonstration of the QZE or the Quantum Anti-Zeno Effect (QAZE), the latter corresponding to the opposite of the QZE and manifesting itself as the speeding up of the system dynamics rather than the slowing down.

Different manifestations of the QZE and QAZE exist beyond a scenario of frequent projective measurements, such as repeated unitary kicks through strong continuous coupling or fast oscillations, and also via strong damping or dynamic decoupling, also known as big-bang decoupling [3]. The QZE and QAZE typically materialise through the reduced decay rate of an unstable quantum system, a decreased rate of quantum tunnelling or the suppression of coherent evolution [4–7]. The first experimental realisation of the QZE was performed by Itano et al. using beryllium ions in a Penning trap [8]. As the frequency of measurements was increased, the probability for the ion to decay from an excited state to the ground state decreased.

A notable motivation for understanding the QZE is that it might be used to stabilise quantum systems in a particular state such that properties of the system such as entanglement and coherence might be maintained [9, 10]. The stability of such properties is of great importance in quantum error correction algorithms or quantum teleportation, as well as in many other quantum computational fields [11–14]. A recent use of the QZE was demonstrated by Blumenthal et al. [15]. It was shown that the joint evolution of at least two non-interacting qubits could be achieved through the continuous measurement of one qubit, such that the operation becomes a multi-qubit entangling gate. A similar effect was found by Nodurft et al. whereby polarisation entanglement could be generated between two initially unentangled photons in coupled waveguides through the QZE [16]. Finally, the QZE has been frequently studied in electron spins in quantum dots, trapped ions and nuclear spins, and Markovian and non-Markovian open quantum system dynamics [17-20].

The difficulty with studying the QZE is that the conventional quantum mechanical framework consists of two distinct regimes. The unitary time evolution of the quantum system governed by the internal Hamiltonian is described by the deterministic, time-reversal symmetric Schrödinger equation, whilst measurement of the quantum system is introduced as an interruption of the unitary evolution of the quantum system in a discontinuous, indeterministic and irreversible manner via the Born rule [21]. As such, the transition of a quantum system from unitary evolution to projection onto a single eigenstate is a nebulous and poorly understood process, often characterised as The Quantum Measurement Problem [21]. Moreover, since the possible future state of a monitored quantum system cannot be determined with certainty from its present state, expectation values of observables are considered

to be the most meaningful properties of a quantum system as opposed to single measurement outcomes, delivering a framework from which statistical averages can be computed but where individual measurements hold less relevance [22].

The (reduced) system density matrix is the principal mathematical tool for calculating such statistical averages. It is often regarded as equivalent to a probability distribution over an ensemble of pure quantum states, such that the reality of the individual stochastic trajectories that might underpin the behaviour is often questioned [23]. As a result, tracking the evolution of a quantum system through a series of measurements (also known as a quantum trajectory) is not a conceptually settled matter. With the consequences of measurement of the system being absent from the dynamical equation of motion, it is not straightforward to characterise the transition from unitary evolution to wavefunction collapse in a clear and explicit manner.

Many techniques for studying the dynamics of open quantum systems exist, such as projection operator methods, Heisenberg equations of motion and the Feynman-Vernon path integral formalism [24–26]. One frequently used method involves quantum master equations, the Lindblad master equation being particularly ubiquitous [27]. Whilst the Lindblad master equation offers much insight into the average evolution of a quantum system interacting with its environment, it cannot reveal the effects of measurement on a quantum system since the state adopted after measurement is obscured in the statistical averaging process [28]. Typically, quantum mechanics is used to describe the evolution of mean quantities (expectation values) as opposed to individual events, and the Lindblad equation performs an average across all possible quantum trajectories brought about by an environment, to deliver an average evolution for the quantum system. Approaches exist where individual trajectories are employed to generate the evolution of the (environmentally-averaged) density matrix, but often these are not regarded as physically realistic: for example the Stochastic Liouville-von Neumann equation is based on an evolving ensemble of density matrices that do not preserve unit trace and thus are not physically meaningful [24].

To reveal the effects of measurement on a system's unitary evolution, an approach that enables the study of single, physically realistic quantum trajectories is required. Quantum State Diffusion (QSD), also known as weak measurement [29], is a framework that offers continuous quantum trajectories and a dynamical treatment of measurement instead of instantaneous wavefunction collapse. QSD considers quantum systems that are in contact with an environment that causes the system density matrix to diffuse across its parameter space. Environmental effects in QSD can drive phenomena such as decoherence and the (continuous) collapse of the system to a particular eigenstate, all within a single dynamical framework. An average over all possible diffusive trajectories then yields the average evolution of the density matrix of the quantum system as given by the Lindblad equation, at least

for Markovian dynamics.

For our purposes, we consider the environment to represent a measuring apparatus, and the strength of the interaction between the quantum system and environment to be a measurement coupling that brings about the diffusion of the system towards a stochastically selected eigenstate. Rather than the system collapsing discontinuously to an eigenstate, as is the case with projective measurements, the measurement process occurs in a continuous and non-instantaneous manner. An approximation to instantaneous wavefunction collapse is obtained in the limit of infinitely strong system-environment coupling. The QSD evolution equation for the system therefore contains not only the unitary time evolution brought about, for example, by a system Hamiltonian, but also the effect of measurement.

The probabilistic nature of the measurement process is represented as stochastic noise in the QSD framework, generating dynamics described by stochastic differential equations (SDEs) or Itô processes when the stochasticity is Markovian [29]. Thus the dynamical consequences of measurement and the intrinsic Hamiltonian time evolution can be studied simultaneously. The trajectories obtained for the evolution of the quantum system are able to offer insight into how and when it arrives at a particular eigenstate, and these are aspects of the QZE. Within such a framework we consider the stochastically evolving density matrix to be a physically real property of the quantum system, instead of merely a tool to calculate the average evolution or representing the state of our knowledge [23, 30]. Nevertheless, results obtained from QSD are consistent with the Born rule, and are therefore compatible with the axioms of quantum mechanics.

One further aspect of such a framework is that the evolution might be interpreted as pseudo-random rather than truly indeterministic since the noise introduced into the system dynamics could be a reflection of the underspecified state of the environment with which the system is interacting, rather like the noise experienced by an open system in classical mechanics. The probabilistic nature of the quantum measurement process, and thus the stochastic evolution of the density matrix, could be due to incomplete control over the state of such an environment. As a result, QSD could help to reveal deterministic features of quantum mechanics. Whether or not we employ this interpretation, the system in QSD resembles a Brownian particle under the influence of probabilistically determined environmental interactions.

Originally formulated in the field of quantum optics by Carmichael et al., quantum trajectories remained an uncharted territory for a long period after the advent of quantum mechanics [31]. This was because the notion of quantum trajectories challenged many of the implications of the Copenhagen interpretation [30, 32, 33], where features pertaining to reality such as causality, determinism and continuity were questioned and replaced with instantaneous and discontinuous quantum jumps and indeterminism. The picture of a quantum system diffusing through points in

the Hilbert space that did not pertain to the possible eigenstates of the observable would have been viewed as unacceptable [28, 32, 33]. It is somewhat unsurprising that the theory's greatest critic, Einstein, had in fact attempted to create a deterministic 'hiddenvariable' quantum trajectory theory in 1927 which was then withdrawn from publication as a result of the discovery of an apparent flaw in the theory [34].

Schrödinger was also known to be doubtful of quantum jumps. He spoke of how 'the current view, which privileges the 'sharp energy states', is selfcontradictory' and how quantum jumps contain 'one great deficiency: while describing minutely the socalled 'stationary' states which the atom had normally, [...] the theory was silent about the periods of transition or 'quantum jumps' (as one then began to call them). Since intermediary states had to remain disallowed, one could not but regard the transition as instantaneous' [33]. Furthermore, the real part of the Schrödinger equation, namely the quantum Hamilton-Jacobi equation, has been developed into a quantum trajectory theory by Dirac, and the de Broglie-Bohm Pilot-Wave theory has offered a deterministic approach to deriving quantum trajectories, whereby randomness is associated with the underspecified initial states of the guiding wave [29, 30, 35-38]. Aside from homodyne and heterodyne experimental measurements, quantum trajectories were observed experimentally by Murch et al. in 2013 in a system where the wavefunction collapse of a superconducting quantum system, initially in a superposition state, was observed by tracking its trajectory in response to a series of weak measurements [39–42]. It appears that there is much to be gained from studying quantum trajectories, beyond a better understanding of the quantum measurement process, and investigating the Quantum Zeno Effect is one such example [43– 45].

Snizhko et al. recently illustrated, through the study of quantum trajectories, that the QZE includes a number of transition stages starting with the system occupying a finite-size region of forbidden states, followed by the introduction of singularities in the steady-state probability distribution of states, and finally an increase in the qubit survival probability [28]. Gambetta et al. also studied the QZE of a superconducting charged qubit coupled to a transmission line resonator with a Rabi control drive, undergoing weak homodyne measurements, using quantum trajectories that illustrated the competition between the measurement drive and the Rabi oscillation system dynamics [46]. As a result of quantum fluctuations the qubit was seen to exhibit jump-like behaviour as the measurement strength increased, transitioning from one eigenstate to the next and, in the limit of large measurement strength, remaining fixed at the same eigenstate for large periods of time, such that the QZE is exhibited. This approach interprets the quantum fluctuations or noise as stemming from a measurement uncertainty much like in classical measurement theory, and, rather than interpreting the quantum trajectories to be objective and independent of any observer, they are taken to be the system state conditioned on

the measurement of the environment [22, 46, 47]. In short, the study of quantum trajectories has elucidated a deeper understanding of the QZE and has also opened up the possibility of quantum system manipulation such as continuous feedback control, entanglement distillation and entanglement phase transitions, phenomena to which the average system evolution is blind [12, 48–51].

In this study of the QZE, we employ QSD to study spin 1/2, spin 1 and spin 3/2 systems, each undergoing Rabi oscillations while coupled to a measuring device that monitors the component of spin along the z-axis. We derive stochastic differential equations for the 'expectation values' of the three Cartesian components of the spin operator, but reinterpret these quantities as stochastic properties of the system associated with individual quantum trajectories as opposed to averages over multiple realisations of the noise or equivalently over an ensemble of adoptable density matrices. The quantum trajectories of each of these systems are used to observe the effects of increased measurement coupling on the unitary dynamics of the system. In particular, the stochastic quantum trajectories are analysed to calculate the probabilities of system residence in the vicinity of z-spin eigenstates, and the average time taken by the system to return to such an eigenstate, and how these quantities depend on the measurement coupling constant.

The plan for the paper is as follows. Section II summarises the key ideas of QSD and SDEs, and Section III provides a specification of the parametrisation and dynamics of the spin systems. Section IV describes the quantum trajectories obtained using such a framework and through an analysis of such trajectories presents insights into the QZE. Our conclusions are given in Section V.

II. QUANTUM STATE DIFFUSION AND A STOCHASTIC LINDBLAD EQUATION

A. Open Quantum Systems and the Kraus Operator Formalism

Open quantum systems are ubiquitous since most systems can be found interacting with their environment. The complexity of this interaction as well as uncertainty in the initial state of the environment mean that an element of randomness enters into the description of the environment's influence on a quantum system. This motivates a description of the open quantum system using a randomly evolving (reduced) density matrix, whose motion mimics that of a Brownian particle diffusing across a phase space.

In order to develop these ideas, consider the commonly used evolution of the density matrix $\rho(t)$ defined through the action of the super-operator $S[\rho]$. Such a map between states of the quantum system must preserve the unit trace and positivity for the quantum state to be considered physically meaningful [52]. The action of such a super-operator on ρ can be expressed as

$$S[\rho] = \sum_{k} M_k \rho(t) M_k^{\dagger} = \sum_{k} p_k(t) \frac{M_k \rho(t) M_k^{\dagger}}{Tr(M_k \rho(t) M_k^{\dagger})}.$$
(1)

The Kraus operators M_k represent all possible transitions brought about by the system dynamics together with system-environment interactions. The Kraus operators can in principle be derived from terms in the Hamiltonian. In order to be trace preserving, they must satisfy the completeness relation $\sum_k M_k^{\dagger} M_k = \mathbb{I}$. One possible interpretation of Eq. (1) is that trans

One possible interpretation of Eq. (1) is that transitions from $\rho(t)$ to $M_k\rho(t)M_k^{\dagger}/Tr(M_k\rho(t)M_k^{\dagger})$ occur with a probability $p_k = Tr(M_k\rho(t)M_k^{\dagger})$ that depends on the density matrix of the system at time t. Stochastic quantum trajectories might then be generated through a series of transitions employing a sequence of Kraus operators. This is a strategy that has been used in studies of evolving quantum systems.

Indeed, to reflect the evolving uncertainty in the state of the quantum system, it would be natural to consider an ensemble of randomly evolving density matrices, the average of which is denoted by the over-bar, $\bar{\rho}$. The evolution of the ensemble averaged density matrix over a time increment dt would then be expressed as [53]

$$\bar{\rho}(t+dt) = \sum_{k} M_k \bar{\rho}(t) M_k^{\dagger}.$$
 (2)

In contrast, the action of a single Kraus operator on a member $\rho(t)$ of such an ensemble represents one of a set of possible system evolutions:

$$\rho(t+dt) = \rho(t) + d\rho = \frac{M_k \rho(t) M_k^{\dagger}}{Tr(M_k \rho(t) M_k^{\dagger})}.$$
 (3)

If such actions are to generate physical trajectories, $\rho(t+dt)$ must remain completely positive and trace preserving. The action of a single Kraus operator can in some circumstances be acceptable in this respect. Consider a density matrix $\rho(t)$ at a time t, specified to be completely positive and hence to have only non-negative eigenvalues. The determinant of such a density matrix is denoted as $\det(\rho(t))$, with $\det(\rho(t)) = \prod_i \lambda_i$ where λ_i denote the eigenvalues of $\rho(t)$. The determinant of $\rho(t)$ is thus positive. Now we consider the determinant of the density matrix at time t+dt, namely $\rho(t+dt)$ generated according to Eq. (3) by a Kraus operator of the form $M = C(\mathbb{I} + A)$ where A is infinitesimal (in the sense that $A \to 0$ as $dt \to 0$) and C is a constant, such that $\tilde{M} = M/C = \mathbb{I} + A$ differs infinitesimally from the identity I. We write

$$\rho(t+dt) = \frac{\tilde{M}\rho(t)\tilde{M}^{\dagger}}{Tr(\tilde{M}\rho(t)\tilde{M}^{\dagger})},\tag{4}$$

and employ the identity $\det(\exp A) = \exp(TrA)$ such that $\det(\mathbb{I} + A) \approx 1 + Tr(A)$ for infinitesimal A,

whereby

$$\det(\rho(t+dt)) = \frac{\det(\tilde{M})\det(\rho(t))\det(\tilde{M}^{\dagger})}{Tr(\tilde{M}\rho(t)\tilde{M}^{\dagger})}$$

$$\approx \frac{(1+Tr(A))\det(\rho(t))(1+Tr(A^{\dagger}))}{Tr(\tilde{M}^{\dagger}\tilde{M}\rho(t))}$$

$$\approx \frac{(1+Tr(A+A^{\dagger}))\det(\rho(t))}{Tr((\mathbb{I}+A+A^{\dagger})\rho(t))}$$

$$= \frac{(1+Tr(A+A^{\dagger}))\det(\rho(t))}{1+Tr(A+A^{\dagger})\rho(t))}$$

$$\approx \det(\rho(t))[1+Tr(A+A^{\dagger})$$

$$-Tr((A+A^{\dagger})\rho(t))]. \tag{5}$$

Next we note that an unacceptable map would produce a density matrix with at least one negative eigenvalue. We can therefore identify unphysical dynamics if a density matrix is generated whose determinant vanishes at some point in time. This includes cases where an odd number of eigenvalues change sign simultaneously (such that the determinant becomes negative) or where an even number do so (such that the determinant goes through a cusp at zero).

So let us examine the dynamics represented by Eq. (5). It can be demonstrated that the determinant of $\rho(t+dt)$ can never go to zero within a finite time-frame, under certain conditions. We express the change in the determinant of the density matrix $d \det(\rho) = \det(\rho(t+dt)) - \det(\rho(t))$ as an Itô process: $d \det(\rho) = \det(\rho)(adt+bdW)$, where dW is a Wiener increment and a and b are functions, obtained through recognising that A is infinitesimal and stochastic (corresponding to various choices of Kraus operator). Letting $y = \ln(\det(\rho))$, the following SDE for y may be obtained:

$$dy = \frac{1}{\det(\rho)} d \det(\rho) + \frac{1}{2} b^2 \det(\rho)^2 \left(-\frac{1}{\det(\rho)^2} \right) dt$$
$$= adt + bdW - \frac{1}{2} b^2 dt. \tag{6}$$

The unacceptable behaviour $\det(\rho) \to 0$ corresponds to $y \to -\infty$ and unless a or b possess singularities it is clear that this can only emerge, if at all, as $t \to \infty$. Thus the dynamics of the single Kraus operator map, Eq. (3), with $M_k = C(\mathbb{I} + A_k)$ and employing a nonsingular, infinitesimal A, are physically acceptable.

We therefore use a set of Kraus operators $M_{\pm k} = \frac{1}{\sqrt{N}}(\mathbb{I} + A_{\pm k})$, where N is the number of Kraus operators in the set $\{M_{\pm k}\}$ and $A_{\pm k} = -iH_sdt - \frac{1}{2}L_k^{\dagger}L_kdt \pm L_k\sqrt{dt}$ [53]. Such an expression satisfies the completeness relation and yields the following Lindblad equation:

$$d\bar{\rho} = -i[H_s, \bar{\rho}]dt + \sum_k \left(L_k \bar{\rho} L_k^{\dagger} - \frac{1}{2} \{ L_k^{\dagger} L_k, \bar{\rho} \} \right) dt,$$
(7)

where L_k are the Lindblad operators and H_s is the system Hamiltonian. The Lindblad equation captures the *average* evolution of the density matrix under the probabilistic influence of an environment whose state

remains uncertain. The dynamics of a quantum system collapsing to a particular eigenstate under measurement cannot be captured by the Lindblad equation since it represents an average over many possible trajectories as opposed to considering a single trajectory. The effect of measurement on the dynamics is obscured by the averaging. To be able to unveil the effects of measurement on a quantum system, we must instead consider single stochastic trajectories. Formally, this constitutes what is termed unravelling Eq. (7) such that an equation concerning a single member of the ensemble of density matrices $\rho(t)$ can be formulated. We next derive such an equation for $\rho(t)$ in the form of an Itô process.

B. Unravelled Stochastic Lindblad Equation

We unravel the deterministic Lindblad equation by implementing the stochastic evolution of ρ according to the set of available transitions

$$\rho(t+dt) = \frac{M_{\pm k}\rho(t)M_{\pm k}^{\dagger}}{Tr(M_{\pm k}\rho(t)M_{\pm k}^{\dagger})},\tag{8}$$

each adopted with probability $p_{\pm k} = Tr(M_{\pm k}\rho(t)M_{\pm k}^{\dagger})$. The outcome is an Itô process for ρ involving independent Wiener increments dW_k (in the case of more than one Lindblad operator) [53]:

$$d\rho = -i[H_s, \rho]dt + \sum_k \left((L_k \rho L_k^{\dagger} - \frac{1}{2} \{ L_k^{\dagger} L_k, \rho \}) dt + \left(\rho L_k^{\dagger} + L_k \rho - Tr[\rho (L_k + L_k^{\dagger})] \rho \right) dW_k \right).$$

$$(9)$$

Solutions to this equation describe possible stochastic quantum trajectories of the reduced system density matrix ρ , where a single trajectory is associated with a particular realisation of the environmental noise $\{dW_k\}$ [45], or equivalently, an initial environmental state. The ensemble-averaged density matrix $\bar{\rho}$ then corresponds to taking an average over the noise and hence over all possible trajectories and, as a result, Eq. (7) is recovered. If the system were closed instead of open, interactions between the system and the environment would vanish and we would be left with the first term on the right-hand side of the equation; namely the von Neumann equation. A similar stochastic evolution equation for ρ has been derived by Jacobs by analogy with classical measurement theory [22]. Under this approach, however, the noise is interpreted as a quantum fluctuation stemming from the uncertainty in the measurement: a similar approach is taken by Gambetta et al. [46]. In contrast, we consider such a noise to reflect the probabilistic nature of interactions with an underspecified environment causing the quantum system to evolve in a stochastic manner, reminiscent of a Brownian particle diffusing in space and described by a Langevin equation.

III. SYSTEM SPECIFICATION

A. Stochastic Differential Equation Parameters

We consider a spin system with a Hamiltonian given by

$$H_s = \epsilon S_x,\tag{10}$$

where ϵ is a positive constant and the operator S_x represents the x-component of the spin: for example in the case of a spin 1/2 system we have $S_i = \frac{1}{2}\sigma_i$ where σ_i denotes a Pauli spin matrix. The spin operators satisfy the condition $[S_i, S_j] = i\epsilon_{ijk}S_k$ where ϵ_{ijk} is the Levi-Civita symbol. We shall consider cases of spin 1/2, spin 1 and spin 3/2 systems where the matrix representations of the S_x , S_y and S_z operators accordingly have dimensions 2, 3 and 4, respectively. The Hamiltonian in Eq. (10) produces Rabi oscillations, as we shall see.

The desired effect of the environment on the system is that it should act as a measuring apparatus. Diffusive evolution of the system's z-component of spin, to be defined shortly, towards one of the eigenstates of the S_z operator, can be achieved using a single Lindblad operator in Eq. (9) of the form

$$L = \alpha S_z, \tag{11}$$

where the constant α denotes the strength of the interaction between the system and its environment and can be regarded as the measurement coupling constant. Figure 1 illustrates the features of the system and its environment. Utilising the above expressions for the Lindblad operator and the system Hamiltonian in Eq. (9), the following expression is obtained for the evolution of the reduced density matrix of the system:

$$d\rho = -i\epsilon[S_x, \rho]dt + \alpha^2 \left(S_z \rho S_z - \frac{1}{2}(\rho S_z^2 + S_z^2 \rho)\right) dt + \alpha \left(\rho S_z + S_z \rho - 2\langle S_z \rangle \rho\right) dW.$$
(12)

The single Wiener increment dW is a Gaussian noise with a mean of zero and a variance dt, and $\langle S_z \rangle$ is the z-component of spin, defined by $Tr(S_z\rho)$. Note that the latter is not to be confused with the usual quantum expectation value of S_z which in our notation is $Tr(S_z\bar{\rho})$, where $\bar{\rho}(t)$ is the density matrix at time t averaged over all possible quantum trajectories. The expectation value represents an average of a (projectively) measured system property taking into account the quantum mechanical randomness of measurement outcome as well as the range of quantum states that might be adopted by an open system when coupled to an uncertain environment. By extension, $\langle . \rangle = Tr(.\rho)$ could be interpreted as a conditional average projective measurement outcome given a specific stochastically evolving density matrix. But it could instead be regarded simply as a property of the density matrix, and hence of the physical state, and indeed it is spin components such as $\langle S_z \rangle$ that undergo Rabi oscillations.

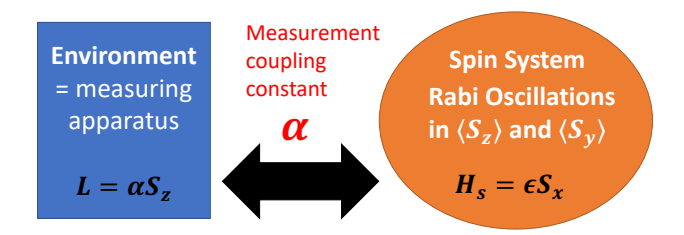


Figure 1. An open quantum spin system interacting with an environment with a strength defined by the coupling constant α . The environment acts as a measurement apparatus, measuring the system's spin along the z-axis.

Terms in Eq. (12) that depend on the measuring coupling constant α represent the effects of measurement on the system, brought about by its interaction with the environment. Notice that for $\epsilon=0$ the stationary states for the measurement dynamics are $\rho=|m_z\rangle\langle m_z|$ where the $|m_z\rangle$ are eigenstates of S_z satisfying $S_z|m_z\rangle=m_z|m_z\rangle$. Starting from an arbitrary initial state, the coupling to the environment captured by the Lindblad operator in Eq. (11) evolves the system towards z-spin eigenstates as desired.

B. Density Matrix Parametrisation

The density matrix of the open quantum system is to be parametrised by a set of variables $\{x_i\}$ which evolve stochastically according to the general Itô processes [54]:

$$dx_i = A_i dt + \sum_j B_{ij} dW_j, \qquad (13)$$

where dW_j denote the Wiener increments and the A_i and B_i are designated functions. The number of parameters required to represent the density matrix depends on the system. Three are required for a density matrix describing a spin 1/2 system, in general. For a spin 1 system, eight parameters are needed since this is the number of independent variables required to specify a 3×3 Hermitian matrix with unit trace. Through a similar reasoning fifteen variables are needed to parametrise the density matrix for a spin 3/2 system.

The density matrix of a spin 1/2 system can be expressed using the Bloch sphere formalism, namely $\rho = \frac{1}{2} (\mathbb{I} + \boldsymbol{r} \cdot \boldsymbol{\sigma})$ with coherence (or Bloch) vector $\boldsymbol{r} = (x,y,z) = Tr(\rho\boldsymbol{\sigma}) = \langle \boldsymbol{\sigma} \rangle$ [55]. SDEs in the form of Eq. (13) can be derived starting from

$$dr_i = Tr(\sigma_i d\rho), \tag{14}$$

with the insertion of Eq. (12). For clarity of presentation, however, we shall employ a one parameter representation for the special case of a pure state with

 $Tr\rho^2 = 1$ or $|\mathbf{r}| = 1$, with coherence vector confined to the (y, z) plane, *i.e.*

$$\rho = \frac{1}{2} (\mathbb{I} + \cos \phi \, \sigma_z - \sin \phi \, \sigma_y), \tag{15}$$

namely x = 0, $y = -\sin \phi$ and $z = \cos \phi$. The SDE for z arising from $dz = Tr(\sigma_z d\rho)$ and Eq. (12) is

$$dz = -\epsilon \sin \phi dt + \alpha \sin^2 \phi dW. \tag{16}$$

The Rabi angle ϕ represents the angle of rotation of the coherence vector about the x axis. In the absence of environmental coupling, the action of the system Hamiltonian $\frac{1}{2}\epsilon\sigma_x$ is to increase ϕ linearly in time. In the presence of such coupling the evolution of the Rabi angle presents an avenue for exploring the effect of measurement on the unitary dynamics of the system. The SDE for $\phi = \cos^{-1}z$ can be found through the use of Itô's lemma [54]:

$$d\phi = \frac{d\phi}{dz}dz + \frac{1}{2}\beta^2 \frac{d^2\phi}{dz^2}dt,$$
 (17)

where $\beta = \alpha \sin^2 \phi$. Inserting Eq. (16) produces

$$d\phi = \left(\epsilon - \frac{1}{4}\alpha^2 \sin 2\phi\right) dt - \alpha \sin \phi dW. \tag{18}$$

When $\alpha = 0$ the Rabi angle increases at a constant rate, while for $\alpha \neq 0$ the Wiener noise dW disturbs its evolution as stated previously. Furthermore, the average rate of change of ϕ is given by

$$\frac{d\langle\phi\rangle}{dt} = \epsilon - \frac{1}{4}\alpha^2\langle\sin 2\phi\rangle,\tag{19}$$

where the brackets again represent an ensemble average. The QZE will emerge if the term proportional to α^2 represents an average retardation of the rotation. In order to resolve this matter we consider the Fokker-Planck equation for p, the probability distribution function (PDF) of the Rabi angle ϕ :

$$\frac{\partial p(\phi, t)}{\partial t} = -\frac{\partial \left(\left(\epsilon - \frac{1}{4} \alpha^2 \sin 2\phi \right) p \right)}{\partial \phi} + \frac{1}{2} \alpha^2 \frac{\partial^2 \left(\sin^2 \phi \, p \right)}{\partial \phi^2}. \tag{20}$$

For small α , an approximate stationary PDF may be obtained:

$$p_{\rm st}(\phi) \propto 1 + \frac{3\alpha^2}{4\epsilon} \sin 2\phi,$$
 (21)

which shows that the PDF is disturbed further from uniformity by increasing the environmental coupling α , or by reducing ϵ which slows the rate of Rabi oscillation for an isolated system. We shall investigate the shape of the stationary PDF numerically for a range of α in Section IV. For now, let us notice that using this approximation the average needed in Eq. (19) is proportional to

$$\int_0^{2\pi} d\phi \left(1 + \frac{3\alpha^2}{4\epsilon} \sin 2\phi \right) \sin 2\phi \propto \int_0^{2\pi} d\phi \sin^2 2\phi > 0,$$
(22)

so the effect of measurement at small α is indeed a mean retardation of the Rabi oscillations, consistent with the Quantum Zeno Effect.

2. Spin 1

To represent the density matrix of a spin 1 system the generalised Bloch sphere formalism is used. This permits any 3×3 density matrix to be written in terms of the Gell-Mann matrices λ_i through

$$\rho = \frac{1}{3} (\mathbb{I} + \sqrt{3} \mathbf{R} \cdot \boldsymbol{\lambda}), \tag{23}$$

where $\boldsymbol{R}=(s,m,u,v,k,x,y,z)$ is an eight dimensional coherence (or Bloch) vector and the Gell-Mann matrices (see Appendix A) form the elements of the vector $\boldsymbol{\lambda}=(\lambda_1,\lambda_2,\lambda_3,\lambda_4,\lambda_5,\lambda_6,\lambda_7,\lambda_8)$ [56]. The following density matrix is thus employed for the spin 1 system:

$$\rho = \frac{1}{3} \begin{pmatrix} 1 + \sqrt{3}u + z & -i\sqrt{3}m + \sqrt{3}s & \sqrt{3}v - i\sqrt{3}k \\ i\sqrt{3}m + \sqrt{3}s & 1 - \sqrt{3}u + z & \sqrt{3}x - i\sqrt{3}y \\ \sqrt{3}v + i\sqrt{3}k & \sqrt{3}x + i\sqrt{3}y & 1 - 2z \end{pmatrix}.$$
(24)

Stochastic quantum trajectories can be produced from the equations of motion for the eight variables parametrising such a density matrix. As before, these are generated from

$$dR_i = \frac{\sqrt{3}}{2} Tr(d\rho \lambda_i), \qquad (25)$$

using the properties of the Gell-Mann matrices, and are specified in Appendix B. The components of the coherence vector \mathbf{R} are denoted R_i .

3. Spin 3/2

In order to construct the density matrix of the spin 3/2 system, an obvious representation would be to utilise SU(4) generators in the generalised Bloch sphere representation:

$$\rho = \frac{1}{4} (\mathbb{I} + \boldsymbol{s} \cdot \boldsymbol{\Sigma}). \tag{26}$$

The 15 component coherence vector is s = (v, e, f, g, h, j, k, l, m, n, o, p, q, s, u) and the vector of generators Σ has components Σ_k with k = 1, 15. However, Aerts and Sassoli de Bianchi discuss how such a representation beyond the SU(2) generators could potentially allow the system to explore unphysical states [55]. Instead, we use Eq. (26) with generators Σ_k constructed using the tensor product of two Pauli matrices: $\Sigma_k = \sigma_i \otimes \sigma_j$: full details are given in Appendix C. The following density matrix is then obtained for the spin 3/2 system:

$$\rho = \frac{1}{4} \begin{pmatrix} 1 + f + p + u & -ie + q - is + v & g + k - il - io & h - ij - im - n \\ ie + q + is + v & 1 - f + p - u & h + ij - im + n & g - k - il + io \\ g + k + il + io & h - ij + im + n & 1 + f - p - u & -ie - q + is + v \\ h + ij + im - n & g - k + il - io & ie - q - is + v & 1 - f - p + u \end{pmatrix}.$$
(27)

As before, stochastic quantum trajectories can be produced from the equations of motion of the 15 variables parametrising the density matrix. SDEs for components of the coherence vector s_k are obtained through

$$ds_k = Tr(d\rho \Sigma_k), \tag{28}$$

and the details can be found in Appendix D.

C. Spin Component Stochastic Differential Equations

The stochastic trajectories of the variables parametrising the density matrices introduced for the spin quantum systems enable us to describe the system dynamics exactly, but do not offer much direct physical insight into the QZE. A more useful way of visualising the behaviour of such systems is to consider the evolution of the time dependent quantities $\langle S_x \rangle$, $\langle S_y \rangle$ and $\langle S_z \rangle$. Recall that these could be interpreted as average values under projective measurements, hence a set of statistics of the dynamics, though we prefer to regard them as

actual physical properties of the current quantum state. It is these quantities that perform noisy Rabi oscillations and we shall refer to them simply as spin components. Two methods exist to determine their evolution.

The first method simply employs $\langle S_i \rangle = Tr(S_i\rho)$ such that the spin components S_i can be written in terms of the aforementioned variables parametrising the density matrices in Eqs. (15), (24) and (27). Alternatively, by considering $d\langle X \rangle = Tr(Xd\rho)$, where operators X are various functions of the S_i , the SDEs that govern the evolution of the spin components can be found using Eq. (12) and solved. We consider these approaches for the three spin systems in turn.

1. Spin 1/2

For the special case density matrix in Eq. (15) the spin components $\langle S_y \rangle$ and $\langle S_z \rangle$ can be written in terms of the Rabi angle $\phi(t)$ as follows:

$$\langle S_y \rangle = -\frac{1}{2} \sin \phi, \qquad \langle S_z \rangle = \frac{1}{2} \cos \phi, \qquad (29)$$

so the phase space explored by $\langle S_y \rangle$ and $\langle S_z \rangle$ is a circle of radius 1/2. We expect a typical stochastic trajectory to dwell increasingly in the vicinity of the z-spin eigenstates at $\phi=0$ and π as the measurement strength increases, and will demonstrate this in Section IV. We also expect the mean rate of passage between the two eigenstates to reduce as the measurement strength increases.

Using a general density matrix $\rho = \frac{1}{2} (\mathbb{I} + \mathbf{r} \cdot \boldsymbol{\sigma})$, the following three SDEs describe the spin components:

$$\begin{split} d\langle S_z \rangle &= \epsilon \langle S_y \rangle dt + 2\alpha \left(\frac{1}{4} - \langle S_z \rangle^2 \right) dW \\ d\langle S_x \rangle &= -\frac{\alpha^2}{2} \langle S_x \rangle dt - 2\alpha \langle S_z \rangle \langle S_x \rangle dW \\ d\langle S_y \rangle &= -\epsilon \langle S_z \rangle dt - \frac{\alpha^2}{2} \langle S_y \rangle dt - 2\alpha \langle S_z \rangle \langle S_y \rangle dW. \end{split} \tag{30}$$

For $\alpha=0$ we clearly see the emergence of Rabi oscillations in $\langle S_y \rangle$ and $\langle S_z \rangle$. Similarly, for $\epsilon=0$ we identify stationary states at $\langle S_x \rangle = \langle S_y \rangle = 0$ and $\langle S_z \rangle = \pm 1/2$, which correspond to the measurement eigenstates.

It may be shown that the purity of the system defined by $P = Tr(\rho^2)$ satisfies

$$dP = \alpha^2 (1 - r_z^2) (1 - P) dt + 2\alpha r_z (1 - P) dW, (31)$$

such that purity moves towards P = 1 and stays there

under the given dynamics. Furthermore, $\langle S_x \rangle = 0$ is a fixed point of the dynamics of Eq. (30) so the special case considered in Eq. (15) describes a more general asymptotic behaviour.

Similarly, the spin components $\langle S_x \rangle$, $\langle S_y \rangle$ and $\langle S_z \rangle$ can be written in terms of the variables parametrising the density matrix in Eq. (24):

$$\langle S_x \rangle = \sqrt{\frac{2}{3}}(x+s)$$

$$\langle S_y \rangle = \sqrt{\frac{2}{3}}(m+y)$$

$$\langle S_z \rangle = \frac{u}{\sqrt{3}} + z.$$
(32)

The purity P of the system can be written

$$P = Tr(\rho^2) = \frac{2}{3}(s^2 + m^2 + u^2 + v^2 + k^2 + x^2 + y^2 + z^2) + \frac{1}{3},$$
(33)

and this evolves asymptotically to unity. The dynamics in terms of spin components and related quantities take the form of eight coupled stochastic differential equations:

$$\begin{split} d\langle S_z \rangle &= \epsilon \langle S_y \rangle dt + 2\alpha \left(\langle S_z^2 \rangle - \langle S_z \rangle^2 \right) dW \\ d\langle S_x \rangle &= -\frac{\alpha^2}{2} \langle S_x \rangle dt + \alpha \left(\langle S_z S_x \rangle + \langle S_x S_z \rangle - 2 \langle S_z \rangle \langle S_x \rangle \right) dW \\ d\langle S_y \rangle &= -\epsilon \langle S_z \rangle dt - \frac{\alpha^2}{2} \langle S_y \rangle dt + \alpha \left(\langle S_z S_y \rangle + \langle S_y S_z \rangle - 2 \langle S_z \rangle \langle S_y \rangle \right) dW \\ d\langle S_y^2 \rangle &= -\epsilon \left(\langle S_y S_z \rangle + \langle S_z S_y \rangle \right) dt - \alpha^2 \left(i \langle S_x S_y S_z \rangle + \langle S_z^2 \rangle + \langle S_y^2 \rangle - 1 \right) dt + \alpha \langle S_z \rangle \left(1 - 2 \langle S_y^2 \rangle \right) dW \\ d\langle S_z^2 \rangle &= \epsilon \left(\langle S_y S_z \rangle + \langle S_z S_y \rangle \right) dt + 2\alpha \langle S_z \rangle \left(1 - \langle S_z^2 \rangle \right) dW \\ d\langle \langle S_y S_z \rangle + \langle S_z S_y \rangle) &= 2\epsilon \left(\langle S_y^2 \rangle - \langle S_z^2 \rangle \right) dt - \frac{\alpha^2}{2} \left(\langle S_y S_z \rangle + \langle S_z S_y \rangle \right) dt + \alpha \left(\langle S_y \rangle - 2 \langle S_z \rangle \left(\langle S_y S_z \rangle + \langle S_z S_y \rangle \right) \right) dW \\ d\langle \langle S_z S_x \rangle + \langle S_x S_z \rangle) &= -\frac{\alpha^2}{2} \left(\langle S_x S_z \rangle + \langle S_z S_x \rangle \right) dt + \alpha \left(\langle S_x \rangle - 2 \langle S_z \rangle \left(\langle S_x S_z \rangle + \langle S_z S_x \rangle \right) \right) dW \\ d\langle S_x S_y S_z \rangle &= i\epsilon \left(\langle S_y S_z \rangle + \langle S_z S_y \rangle \right) dt + i\alpha^2 \left(\langle S_z^2 \rangle + 2i \langle S_x S_y S_z \rangle \right) dt + i\alpha \langle S_z \rangle \left(1 + 2i \langle S_x S_y S_z \rangle \right) dW. \end{split} \tag{34}$$

Again, the regular Rabi dynamics around a circle in the phase space of $\langle S_y \rangle$ and $\langle S_z \rangle$ is apparent when $\alpha = 0$. When $\alpha \neq 0$ the trajectories are more complicated. For $\epsilon = 0$ the eigenstates of the z-spin are stationary: the relevant spin components being $\langle S_x \rangle = \langle S_y \rangle = 0$ and $\langle S_z \rangle = \pm 1, 0$.

Once again, the spin components can be written in terms of the variables parametrising the density matrix for the spin 3/2 system in Eq. (27) as follows:

$$\langle S_x \rangle = \frac{1}{2}(h+n+\sqrt{3}v)$$

$$\langle S_y \rangle = \frac{1}{2}(\sqrt{3}e-j+m)$$

$$\langle S_z \rangle = \frac{1}{2}f+p.$$
(35)

The purity of the system P may be written

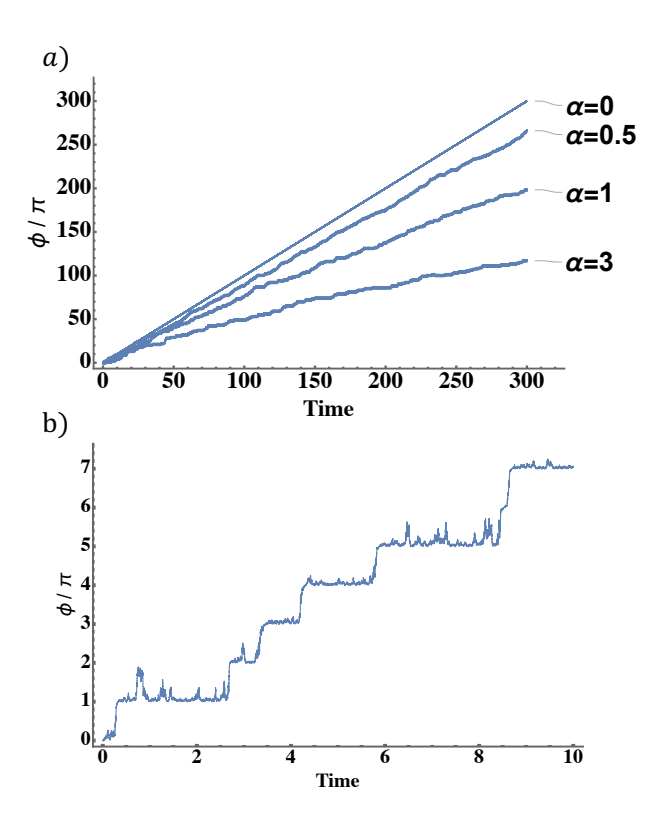


Figure 2. a) The evolution of the Rabi angle ϕ for a spin 1/2 system at four values of α with time-step 0.0005, $\epsilon=1$ and a duration of 300 time units. The mean rate of change is reduced as the strength of measurement is increased. b) Close-up of the evolution of ϕ for $\alpha=1$ for a duration of 10 time units. Notice that for this strength of measurement the Rabi angle tends to dwell in the vicinity of integer multiples of π , the z-spin eigenstates.

$$P = \frac{1}{4} \left(1 + e^2 + f^2 + g^2 + h^2 + j^2 + k^2 + l^2 + m^2 + n^2 + o^2 + p^2 + q^2 + s^2 + u^2 + v^2 \right).$$
(36)

For the spin 3/2 system a closed set of fifteen stochastic differential equations for the spin components and related quantities could not be found. Thus Eqs. (35) and the SDEs in Appendix D are the only way to solve the dynamics for this spin system.

IV. SIMULATIONS AND RESULTS

A. Spin 1/2

The equations of motion for the variables parametrising the density matrices of the spin 1/2, spin 1 and spin 3/2 systems, given by Eqs. (18), (25) and (28), were solved numerically using the Euler-Maruyama update method [57]. From the evolution of these variables, stochastic quantum trajectories in the phase space of the z-spin component $\langle S_z \rangle$ and the y-spin component $\langle S_y \rangle$ were produced. For spin 1/2 we also generated stochastic trajectories of the Rabi angle ϕ . We chose the x-spin component to be zero initially, where it remains.

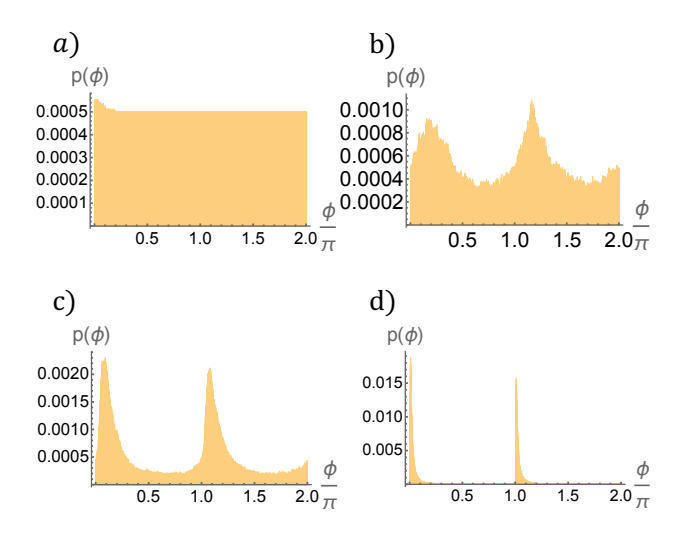


Figure 3. Stationary probability density functions for the Rabi angle in the spin 1/2 system, for the following measurement coupling constants α , obtained over a duration of 300 time units with a time-step of 0.0005 and $\epsilon=1$. a) $\alpha=0$, b) $\alpha=0.5$, c) $\alpha=1$, d) $\alpha=3$. The eigenstates of S_z lie at $\phi=0$ and at $\phi=\pi$. Notice the displacement of the peaks above the eigenvalues, arising from the pull of the Hamiltonian.

The evolution of the Rabi angle with time for the spin 1/2 system for various strengths of measurement is shown in Figure 2. Figure 2a shows that the mean rate of change of the Rabi angle, namely the mean frequency of Rabi oscillations, decreases with increasing measurement coupling constant, as was suggested by Eq. (19). Such a decrease demonstrates the slowing down of the unitary dynamics as a result of stronger, or equivalently, more frequent measurement as expected for the QZE. Figure 2b illustrates the dynamics on a finer scale. The quantum jumps conventionally considered to occur between eigenstates of a monitored observable, brought about by an interaction present in the Hamiltonian, can be seen as a coarse-grained (in time) approximation to the underlying continuous dynamics.

Numerically generated stationary PDFs for the Rabi angle are shown in Figure 3 for an isolated system ($\alpha = 0$) and for three nonzero measurement strengths. Initial states were selected from a uniform probability density over ϕ . Angles $\phi=0$ and π correspond to the $|\frac{1}{2}\rangle$ and $|-\frac{1}{2}\rangle$ eigenstates of S_z , respectively. Values of ϕ from the trajectories are mapped into the range 0 to 2π . It can be seen that as the measurement strength is increased, the stationary PDFs become narrower since the measurement dynamics are better able to localise the system in the vicinity of the eigenstates of S_z , resisting the pull of the unitary dynamics induced by the Hamiltonian, which seek to drive the system into Rabi oscillations. In accordance with the Born rule, for $\alpha > 0$ the stationary PDFs contain two approximately equivalent peaks around the $\left|-\frac{1}{2}\right\rangle$ and $\left|\frac{1}{2}\right\rangle$ eigenstates, since the system should have an equal probability of localising at either. The PDF in Figure 3a is uniform over ϕ since the trajectories represent the dynamics without measurement, namely Rabi oscillations. Note that the stationary

PDF in Figure 3b is roughly sinusoidal, as suggested by the PDF for small α given in Eq. (21). Indeed, that approximate result suggested peaks at $\phi = \pi/4$ and $3\pi/4$: a consequence of the competition between measurement-induced dwell near the eigenstates and the rotational pull of the Hamiltonian. As measurement strength increases, the peaks are drawn closer to $\phi = 0$ and π .

B. Spin 1

The evolution of $\langle S_z \rangle$ and $\langle S_y \rangle$ for a spin 1 system, for different values of the measurement coupling constant α , is illustrated in Figure 4. The system was initialised in the $|-1\rangle$ spin eigenstate of the S_z operator. Figure 4a illustrates the dynamics when there is no measurement: the Hamiltonian drives Rabi oscillations in $\langle S_z \rangle$ and $\langle S_y \rangle$ corresponding to the precession of the spin vector around the $\langle S_x \rangle$ axis. The $|\pm 1\rangle$ and $|0\rangle$ eigenstates of S_z lie at $\langle S_x \rangle = 0$, $\langle S_y \rangle = 0$ and $\langle S_z \rangle = \pm 1$ and 0, respectively. If the initial state of the system had been the $|0\rangle$ eigenstate of S_z , then the spin vector would lie on the $\langle S_x \rangle$ axis and would be unable to precess around it, and furthermore, $\langle S_z \rangle$ and $\langle S_y \rangle$ would be zero.

Disturbance of the circular trajectories can be seen in Figure 4b. As a result of the nonzero measurement coupling constant the system can now pass near the $|0\rangle$ eigenstate of S_z , located at the origin. As the measurement coupling constant is increased further in Figure 4c-d, a figure-of-eight pathway forms and the system dwells more often at the $|0\rangle$ eigenstate until, in Figure 4e-f, visits to this state always occur in between visits to the $|-1\rangle$ and $|1\rangle$ eigenstates.

Note that the spin 1 system is not moving at a constant speed around these figure-of-eight pathways. Instead, the system makes rapid jumps between the eigenstates, typically in a counter-clockwise direction, separating periods of dwell in the vicinity of the eigenstates. Movies of examples of the spin 1 [58] and spin 3/2 [59] system dynamics are available. The behaviour is illustrated in plots of the relative probability of occupation of patches of the phase space by the system, shown in Figure 5. The behaviour is similar to that of the spin 1/2 system: a greater tendency to localise near the eigenstates as α is increased, while the pull of the Hamiltonian produces a counterclockwise displacement.

Figure 6 further illustrates how increasing the measurement coupling constant causes the system to dwell for longer at the three eigenstates of S_z and transit more abruptly between them. The behaviour at high measurement strength increasingly resembles the traditional textbook behaviour of a system making jumps between eigenstates.

In order to quantify the QZE, we consider the α dependence of two quantities derived from the trajectories in Figure 4. First, the residence probabilities, which characterise the fraction of time spent in the vicinity of each eigenstate of S_z over a long simulation. The system is defined to occupy an eigenstate if the $\langle S_z \rangle$ coordinate lies within ± 0.1 of the appro-

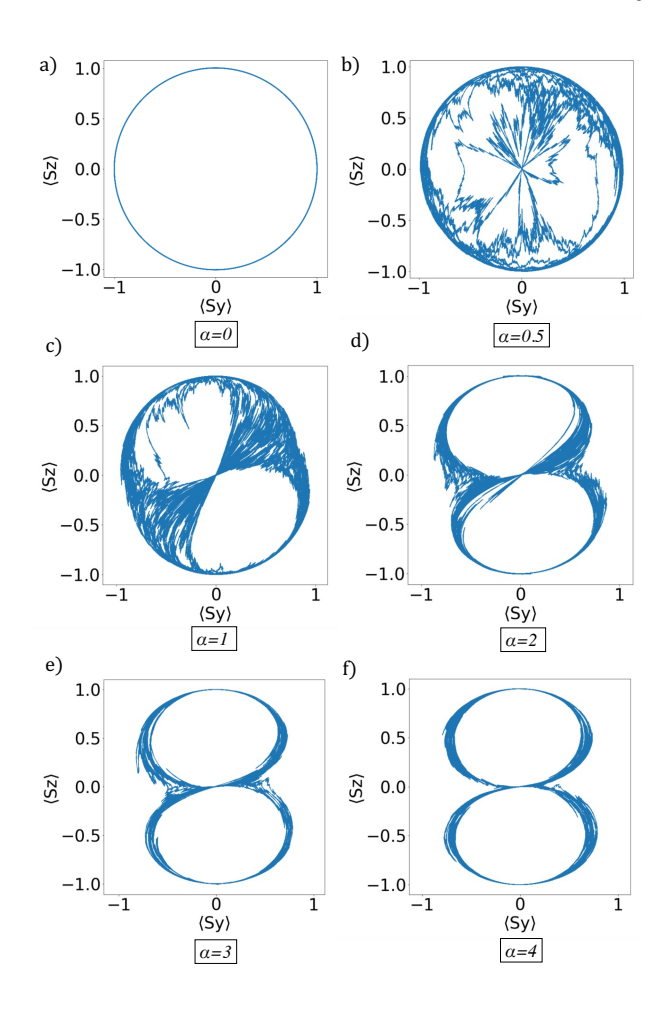


Figure 4. The path taken through $\langle S_y \rangle$, $\langle S_z \rangle$ phase space for a spin 1 system with varying measurement coupling constant α , for $\epsilon=1$, time-step 0.0001 and for a duration of 50 time units. As the strength of measurement increases, the circular path corresponding to regular Rabi oscillations at $\alpha=0$ becomes disturbed, allowing visits to the $|0\rangle$ eigenstate at the origin in addition to the $|\pm 1\rangle$ eigenstates at the top and bottom of the phase space.

priate eigenvalue. The second quantity considered is the mean return time. This is the average period from the moment the system leaves a particular eigenstate (with occupation defined as above) to the moment it returns to it having visited another eigenstate in between.

Figure 7a illustrates how residence probabilities are small for low values of α , which is a reflection of the only slightly disturbed oscillatory behaviour of $\langle S_z \rangle$ in Figure 6a. But as the coupling strength is raised, so do the residence probabilities, and this can similarly be understood by considering the trajectory shown in Figure 6b. Little time is spent in regions far away from the eigenstates. Visits to the $\langle S_z \rangle = 0$ eigenstate are less frequent than to the ± 1 eigenstates for small α , which is a consequence of having started the trajectory at $\langle S_z \rangle = -1$, but they occur with approximately equal probability at high values of α .

Figure 7b shows how the system takes longer times to return to an eigenstate for strong measurement coupling. Again, this is consistent with the behaviour shown in Figure 6b. The return time for a given eigen-

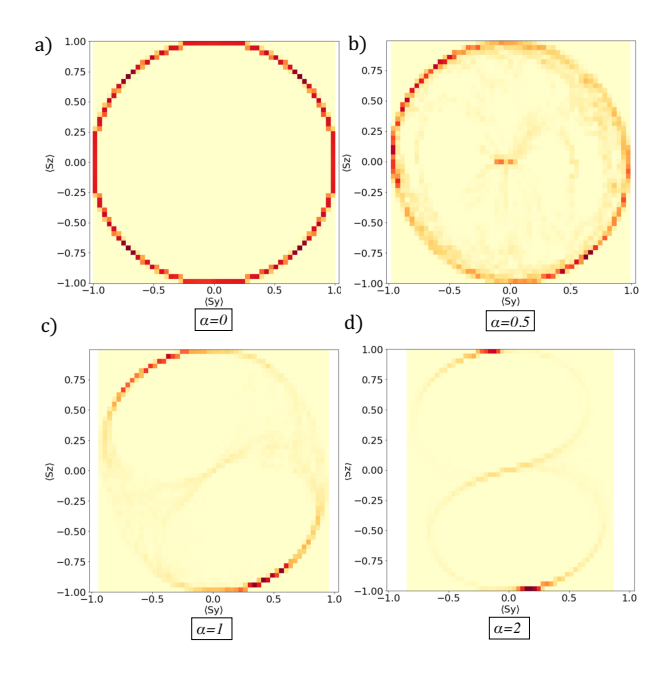


Figure 5. Density plot (51 by 51 bins) illustrating stationary relative occupation in the $\langle S_y \rangle$, $\langle S_z \rangle$ phase space of the spin 1 system for four values of α , obtained from trajectories with a duration of 100 time units, a time-step of 0.0001 and $\epsilon=1$.

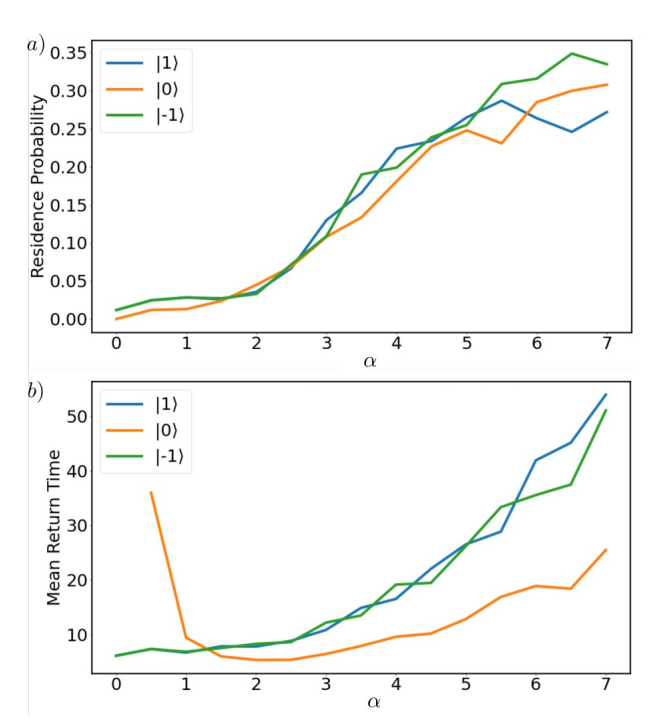


Figure 7. a) Residence probabilities, and b) mean return times for the eigenstates of a spin 1 system, with varying measurement coupling constant α , for $\epsilon=1$, time-step of 0.0001 and for a duration of 5000 time units.

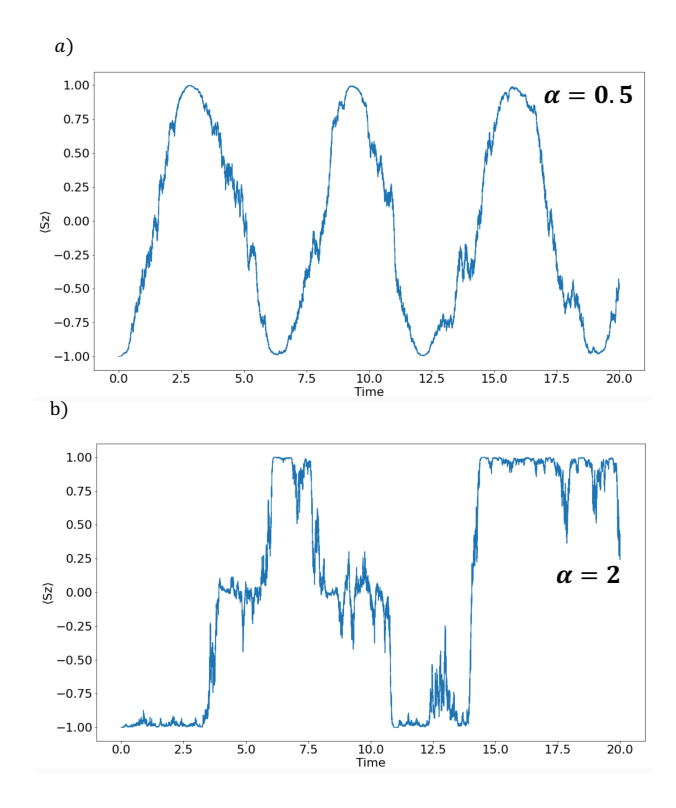


Figure 6. Trajectories of $\langle S_z \rangle$ for the spin 1 system for a) $\alpha=0.5$ and b) $\alpha=2$. Slightly noisy Rabi oscillations at low measurement strength are contrasted with fast jumps between the eigenstates at $\langle S_z \rangle=\pm 1$ and 0, with random waiting times, when the measurement strength is increased.

state is dominated by the period of dwell at the eigenstate (or eigenstates) to which it moves. The return time to the $\langle S_z \rangle = 0$ state initially decreases with α but this is an artefact of the initial condition for the motion, which makes visits to this eigenstate rare when α is small (as is apparent in Figure 4). The return time for the $\langle S_z \rangle = 0$ eigenstate is typically less than the return times for $\langle S_z \rangle = \pm 1$, possibly because direct transitions between the $\langle S_z \rangle = 1$ and -1 states are unlikely. Return to the central eigenstate is characterised by just one period of dwell at one of the two outer eigenstates, while return to an outer eigenstate might require waiting while the system hops between the other two states.

The definition of the vicinity of an eigenstate is, of course, open to debate. The choice we make is simple but is sufficient to reveal the effects that characterise the QZE. It is natural that the value of $\langle S_z \rangle$ should feature prominently in the definition, but there are other characteristics of the eigenstates that could be taken into account. An eigenstate of the S_z operator corresponds to a point in a multidimensional parameter space, and perhaps its vicinity should be defined by putting conditions on some of these additional parameters. We have investigated a more elaborate scheme along these lines but the resulting residence probabilities and mean return times are broadly similar to those shown in Figure 7. In the interests of simplicity we therefore focus on the value of $\langle S_z \rangle$ alone, and the chosen range.

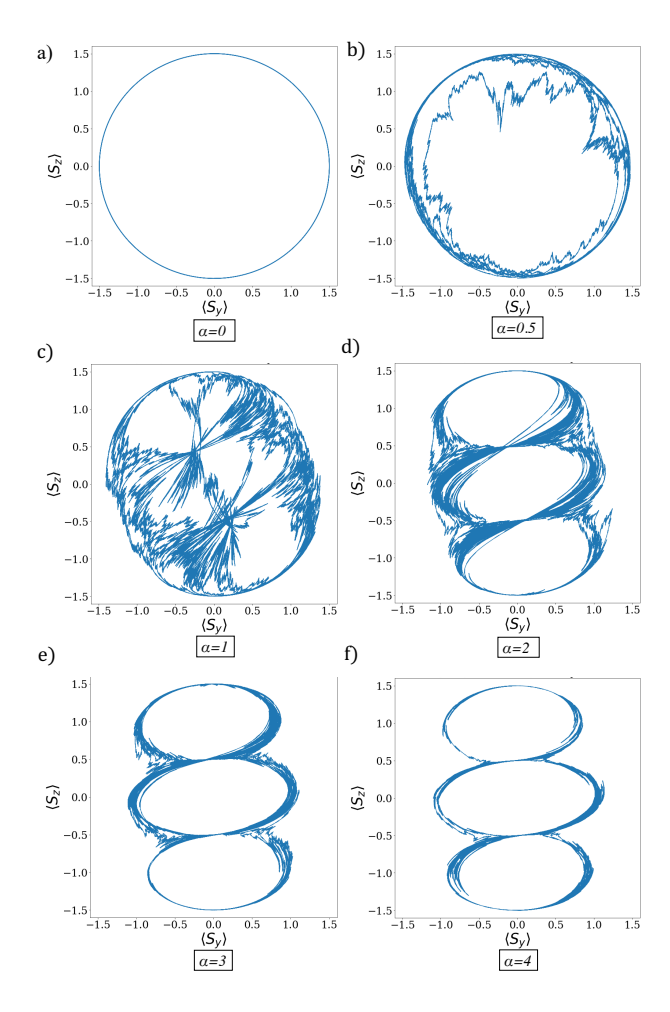


Figure 8. Paths through the $\langle S_y \rangle$, $\langle S_z \rangle$ phase space explored by a spin 3/2 system with varying measurement coupling constant, for $\epsilon=1$, time-step 0.0001 and duration 50 time units.

C. Spin 3/2

The effects of measurement on a spin 3/2 system, viewed in terms of the evolution of spin components $\langle S_z \rangle$ and $\langle S_y \rangle$, is illustrated in Figure 8 for different values of the measurement coupling constant α . The system was initialised in the $\left|-\frac{3}{2}\right\rangle$ eigenstate of S_z . When $\alpha = 0$ there is no measurement and, as with the spin 1 system, the Hamiltonian drives circular trajectories, as depicted in Figure 8a, passing through the $\left|\frac{3}{2}\right\rangle$ and $\left|-\frac{3}{2}\right\rangle$ eigenstates of S_z at $\langle S_y\rangle=0$ and $\langle S_z \rangle = \pm 3/2$. The spin vector precesses around the $\langle S_x \rangle$ axis. As α is increased (Figure 8b-f), the circular trajectory is disturbed such that the system traverses through further regions of phase space, including the vicinities of the $|\frac{1}{2}\rangle$ and $|-\frac{1}{2}\rangle$ eigenstates of S_z at $\langle S_y \rangle = 0$ and $\langle S_z \rangle = \pm 1/2$. When the measurement coupling constant is sufficiently high, a triple figure-of-eight trajectory emerges, such that the $\left|\frac{1}{2}\right>$ and $\left|-\frac{1}{2}\right\rangle$ eigenstates are visited in between visits to the $|\frac{3}{2}\rangle$ eigenstate and the $|-\frac{3}{2}\rangle$ eigenstate, and visaversa. The system dwells in the vicinities of all four eigenstates of S_z for high enough α .

Figure 9a illustrates how the residence probabilities for the spin 3/2 system depend on α . As with the spin

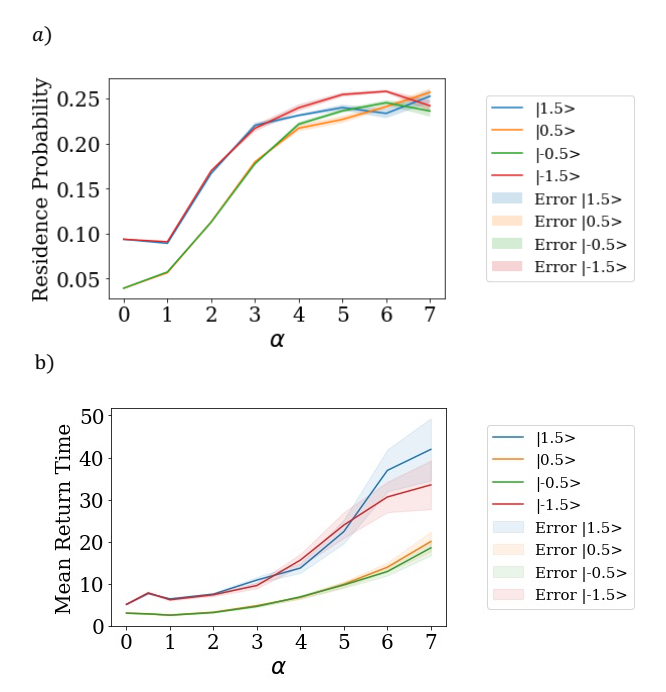


Figure 9. The residence probabilities and mean return times for the eigenstates of a spin 3/2 system, with varying measurement coupling constant α , for $\epsilon=1$, time-step of 0.0001 and for a duration of 5000 time units.

1 case, the system is defined to occupy an eigenstate if the $\langle S_z \rangle$ coordinate lies within ± 0.1 of the appropriate eigenvalue. At low values of α , the Hamiltonian term dominates and therefore occupation of the $|\frac{1}{2}\rangle$ and $|-\frac{1}{2}\rangle$ eigenstates of S_z is lower than for the $|\frac{3}{2}\rangle$ and $|-\frac{3}{2}\rangle$ eigenstates. For higher values of α , the residence probabilities for all four eigenstates increase and become roughly equal, in concord with the Born rule, and a triple figure-of-eight trajectory is followed. For large α , the probability of occupying each eigenstate lies around 0.25, implying that the system is unlikely to occupy a point in the phase space outside the vicinity of the eigenstates. Note that increasing the value of α amplifies the noise term in Eq. (12), introducing greater statistical uncertainty into the simulation.

Figure 9b shows that as the measurement coupling constant is raised the mean return times increase, hence demonstrating the QZE. Notably, the mean return times for the $|\frac{1}{2}\rangle$ and $|-\frac{1}{2}\rangle$ eigenstates of S_z are approximately half those of the $|\frac{3}{2}\rangle$ and $|-\frac{3}{2}\rangle$ eigenstates. When the system resides at the $|\frac{1}{2}\rangle$ and $|-\frac{1}{2}\rangle$ eigenstates, and α is high enough, there are two states to which it can transfer, as opposed to one when it resides at the $|\frac{3}{2}\rangle$ and $|-\frac{3}{2}\rangle$ eigenstates. The $|\pm\frac{1}{2}\rangle$ lie within the ladder of eigenstates while the $|\pm\frac{3}{2}\rangle$ are its termini. Twice the number of paths for a return to $|\frac{1}{2}\rangle$ compared with $|\frac{3}{2}\rangle$ suggests half the mean return time.

We speculate that higher spin systems will continue this pattern of behaviour. Systems with large measurement coupling will follow stochastic transitions along a multiple figure-of-eight pathway in the phase space of $\langle S_z \rangle$ and $\langle S_y \rangle$. The behaviour will evolve from regular Rabi oscillations towards a situation where

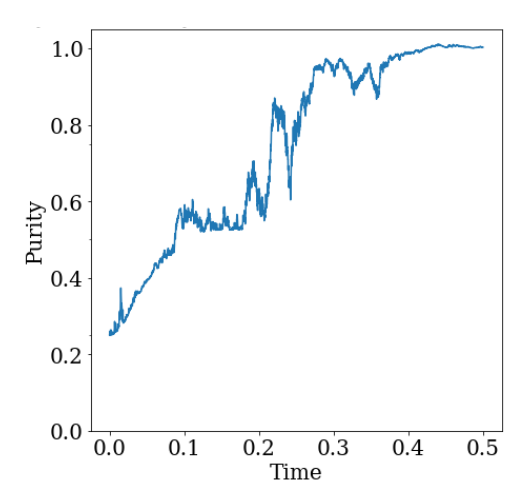


Figure 10. The evolving purity of a spin 3/2 system for a single quantum trajectory, starting from a fully mixed state, with $\alpha=3,~\epsilon=1,$ time-step 0.0001 and for a duration of 0.5 time units.

the system (effectively) jumps stochastically between eigenstates of the monitored observable.

Finally, the evolution of the purity of the spin 3/2 system under measurement was studied to ensure it remained within the expected range of $\frac{1}{4} \leq P \leq 1$, starting with the system in the fully mixed state $\rho = \frac{1}{4}\left(|-\frac{3}{2}\rangle\langle-\frac{3}{2}|+|-\frac{1}{2}\rangle\langle-\frac{1}{2}|+|\frac{1}{2}\rangle\langle\frac{1}{2}|+|\frac{3}{2}\rangle\langle\frac{3}{2}|\right)$. In Figure 10 it can be seen that the effect of measurement is to cause the system to purify, as has previously been claimed. The purification occurs in a continuous but stochastic manner, taking approximately 0.4 time units for the parameters chosen. The approximation of instantaneous projective measurements and apparent jumps in purity emerges only in the limit $\alpha \to \infty$.

It is worth noting that the dynamical framework we use has the effect that interaction brings about a disentanglement of the system from its environment, an increase in purity, which is the opposite of what is often supposed. However, this is an appropriate outcome for measurement, where the idea is to convey the system into a (pure) eigenstate of the appropriate observable. More general system-environment interactions might change the system purity in different ways, but to take this into account would require a more explicit representation of environmental degrees of freedom than that which we have employed.

V. DISCUSSION AND CONCLUSIONS

The Quantum Zeno Effect (QZE) has been studied in three open spin systems undergoing Rabi oscillations generated by Hamiltonian $H_s \propto S_x$ and coupled to an environment designed to act as a measurement apparatus for the S_z observable. The interaction between the system and environment is characterised by a measurement coupling constant α . Under the conventional quantum mechanical framework the measurement process is discontinuous and not included in the dynamical equation of motion of the system. Statistical averages are deemed to be more meaningful than single measurement outcomes. The consequences

of measurement on the unitary dynamics of the quantum system are not easily studied within such a framework. But the quantum state diffusion approach allows the construction of single, physical, stochastic quantum trajectories, and can take into account the effects of measurement in a continuous and explicit manner.

The evolution of an open quantum system is therefore modelled using a stochastically evolving (reduced) density matrix, ρ , preserving the unit trace and positivity. Such trajectories can be considered as physically meaningful, unlike, for example, the trajectories used to solve the Stochastic Liouville-von Neumann equation. The evolution of the quantum system resembles that of a Brownian particle diffusing across a phase space, and the density matrix, at each instant, is interpreted as a physical property of the system. The average over an ensemble of density matrices represented by the stochastic trajectories is captured by the noise-averaged Lindblad equation. The stochasticity in the system dynamics may be interpreted to be pseudo-random and stemming from an under-specified environment as opposed to an intrinsic indeterminism.

Stochastic quantum trajectories for the spin 1/2 system have been described in terms of the evolution of the Rabi angle. For the spin 1 and spin 3/2 systems, the evolution of the 'expectation values' $\langle S_y \rangle = Tr(\rho S_y)$ and $\langle S_z \rangle = Tr(\rho S_z)$ were studied. It is important to note that, in spite of the terminology just used, we regard these spin components as physical properties rather than statistics and that they characterise a single stochastic evolution. To demonstrate the QZE, the spin 1 and spin 3/2 trajectories were analysed to calculate the mean return times under the dynamics, and the residence probabilities, for the various eigenstates of S_z .

The stochastic trajectories for both the spin 1 and spin 3/2 systems (Figures 4 and 8) reveal a competition between the unitary dynamics which attempt to guide the system along a deterministic trajectory in the $\langle S_y \rangle$, $\langle S_z \rangle$ phase space, and the non-unitary measurement dynamics which seek to divert the system stochastically towards the eigenstates of S_z , and dwell in their vicinity. For example, measurement can disturb a deterministic trajectory, passing through eigenstates with the largest eigenvalues, allowing occasional visits to the other eigenstates of S_z , such as the $|0\rangle$ eigenstate in the case of the spin 1 system and $|\frac{1}{2}\rangle$ and $|-\frac{1}{2}\rangle$ in the case of the spin 3/2 system. For high enough values of α , the system traverses a figure-of-eight path in the case of the spin 1 system, and a triple-figure-of-eight path for the spin 3/2 system. We speculate that a similar pattern will be found for higher spin systems, where for very high values of α the system will simply appear to jump stochastically between the eigenstates. As such, the transition pathways available to the quantum system appear to change according to the strength of the measurement imposed upon it. Quantum contextuality, namely, the outcome of a measurement being dependent on what is measured, and demonstrated in experiments such as the quantum eraser or delayed-choice Mach-Zehnder Interferometer, can be extended not only to *what* is being measured, but *how* it is being measured [21, 60–63]. In other words, how strongly the measurement is conducted on a quantum system is able to dictate what states the system is permitted to traverse.

Von Neumann very much saw our continuous experience of reality as illusionary. He wrote that 'the principle of continuity ("natura non facit saltus"), prevailing in the macroscopic world, is merely simulated by an averaging process in a world which in truth is discontinuous by its very nature. [...] The leveling law of large numbers completely obscures the real nature of the individual processes' [64]. But in contrast to von Neumann's view of jumps in quantum mechanics, the purity of a spin 3/2 system, initially in a mixed state, has been demonstrated to increase in a continuous manner and within a finite period of time as a result of measurement (see Figure 10). The trajectories of the spin 1 system in the phase space of $\langle S_z \rangle$ (Figure 6) develop from noisy Rabi oscillations at low values of the coupling constant to relatively abrupt but continuous randomly occurring jumps between the eigenstates of S_z at high values of α , similar to those illustrated in the evolution of the Rabi angle for the spin 1/2 case in Figure 2b. Moreover, the figure-of-eight and triple-figure-of-eight patterns of the spin 1 and spin 3/2 system trajectories, respectively (Figures 4 and 8), depict a continuous dynamics demonstrating that the system is able to pass through points away from the eigenstates of the observable.

In quantum state diffusion, the eigenstates are the points towards which the system diffuses and where it might dwell for the longest stretches of time, rather than being a set of states to which the system path is exclusively confined. For large values of α , there are distinct pathways between the different eigenstates that the system explores when making transitions. Instantaneous quantum jumps can be interpreted as the limiting case for very strong interaction between system and measuring apparatus $(\alpha \to \infty)$. Thus, projective measurements and quantum jumps might be seen as a coarse-graining, in time, of weak measurements, and that this 'obscures the real nature of individual processes'. And it should be noted that if a statistical average is performed over all possible diffusive quantum trajectories, to produce an average density matrix $\bar{\rho}$ as described by the conventional quantum mechanical framework of the Lindblad equation, then this jump behaviour is typically not apparent. The expectation value $Tr(\bar{\rho}S_z)$ is indeed a statistic rather than a physical property.

The stochastic trajectories generated for all three spin systems for a range of values of the coupling constant have clearly demonstrated the QZE. With increasing measurement strength, the mean rate of change of the Rabi angle for the spin 1/2 system decreases (Figure 2a). Since the Rabi angle describes rotation of the coherence/Bloch vector about an axis specified by the Hamiltonian, such a decrease of its mean rate of change demonstrates a slowing down of the unitary dynamics. Suppression of the unitary dynamics was also illustrated by the increased mean return time to eigenstates in the spin 1 and spin 3/2

systems (Figures 7b and 9b). Increased measurement strength causes the system to dwell for longer at each eigenstate, a clear manifestation of the QZE. The stationary PDFs of the spin 1/2 system (Figure 3) show that an increase in coupling constant narrows the PDFs around the eigenstates of S_z .

Probabilities of residence near the eigenstates of S_z for both spin 1 and spin 3/2 systems rise to a ceiling with increasing measurement coupling constant (Figures 7a and 9a). At low values of the coupling constant, the system spends significant time exploring phase space away from the eigenstates of S_z , but, for example, the spin 3/2 residence probabilities for the four eigenstates rise to about 0.25 for $\alpha > 6$. Such a localisation was also demonstrated by the pattern of the stationary probability densities over $\langle S_z \rangle$ and $\langle S_y \rangle$ for spin 1 (Figure 5) such that, for high values of α , the density was almost exclusively confined to regions of phase space in the vicinity of the three eigenstates. The non-unitary measurement dynamics appear to dominate, localising the system near the eigenstates and supporting the conventional picture of wavefunction collapse.

Much of the discussion of quantum trajectories has centred on the extent to which they can be considered realistic [23, 65, 66]. Averaging over such trajectories or over the noise is said to be required since this corresponds to an averaging over the randomness of unobserved, microscopic events. However, our results illustrate that not performing such a statistical average can still yield realistic quantum trajectories and consequences of the measurement process are made more apparent as a result. Not only are the standard results of quantum mechanics obtained, but the phenomenon of QZE is easily observed, and we are able to gain an understanding of how and when the quantum system collapses to an eigenstate.

By treating the measurement process as an interaction between a system and its environment, the distinction between measurement and all other possible interactions between a system and environment appears to dissolve. A measurement becomes merely an environmental interaction that tends to drive the quantum system towards purity, and potentially towards an eigenstate.

Apart from demonstrating the QZE in a simple system, the QSD framework for generating stochastic quantum trajectories could be used to shed light onto other features of quantum systems such as entanglement, decoherence and measurement back-action. It could also reveal behaviour in more complex systems such as those possessing a memory of past environment-system interactions. Whilst the dynamics of some quantum systems might be well approximated by Markovian stochastic trajectories, future work could consider non-Markovian unravellings or non-Markovian master equations generating stochastic trajectories that are not constrained by the Born-Markov approximation, enabling the study of complex environments with non-negligible correlation times.

ACKNOWLEDGMENTS

SMW is supported by a PhD studentship funded by EPSRC under grant codes EP/R513143/1 and EP/T517793/1.

- [1] A. Degasperis, L. Fonda, and G. C. Ghirardi, Does the lifetime of an unstable system depend on the measuring apparatus?, Il Nuovo Cimento A 21, 471 (1974).
- [2] B. Misra and E. C. G. Sudarshan, The Zeno's paradox in quantum theory, Journal of Mathematical Physics 18, 756 (1977).
- [3] I. Georgescu, Quantum Zeno effect at 45, Nature Reviews Physics 4, 289 (2022).
- [4] Y. S. Patil, S. Chakram, and M. Vengalattore, Measurement-Induced Localization of an Ultracold Lattice Gas, Physical Review Letters 115, 140402 (2015).
- [5] J. M. Raimond, P. Facchi, B. Peaudecerf, S. Pascazio, C. Sayrin, I. Dotsenko, S. Gleyzes, M. Brune, and S. Haroche, Quantum Zeno dynamics of a field in a cavity, Physical Review A 86, 032120 (2012).
- [6] B. Yan, S. A. Moses, B. Gadway, J. P. Covey, K. R. A. Hazzard, A. M. Rey, D. S. Jin, and J. Ye, Observation of dipolar spin-exchange interactions with latticeconfined polar molecules, Nature 501, 521 (2013).
- [7] G. Barontini, R. Labouvie, F. Stubenrauch, A. Vogler, V. Guarrera, and H. Ott, Controlling the Dynamics of an Open Many-Body Quantum System with Localized Dissipation, Physical Review Letters 110, 035302 (2013).
- [8] W. M. Itano, D. J. Heinzen, J. J. Bollinger, and D. J. Wineland, Quantum Zeno effect, Physical Review A 41, 2295 (1990).
- [9] M. H. Oliveira, G. Higgins, C. Zhang, A. Predojević, M. Hennrich, R. Bachelard, and C. J. Villas-Boas, Steady-state entanglement generation for non-degenerate qubits (2022), arXiv:2205.10590 [quant-ph].
- [10] H. Salih, J. R. Hance, W. McCutcheon, T. Rudolph, and J. Rarity, Deterministic Teleportation and Universal Computation Without Particle Exchange, arXiv:2009.05564 [quant-ph] (2021).
- [11] Y.-H. Chen and T. A. Brun, Continuous quantum error detection and suppression with pairwise local interactions, Physical Review Research 2, 043093 (2020).
- [12] Y. Li, X. Chen, and M. P. A. Fisher, Quantum Zeno Effect and the Many-body Entanglement Transition, Physical Review B 98, 205136 (2018), arXiv:1808.06134 [cond-mat, physics:quant-ph].
- [13] J.-D. Lin, C.-Y. Huang, N. Lambert, G.-Y. Chen, F. Nori, and Y.-N. Chen, Space-time dual quantum Zeno effect: Interferometric engineering of open quantum system dynamics (2022), arXiv:2208.02472 [quant-ph].
- [14] X. Long, W.-T. He, N.-N. Zhang, K. Tang, Z. Lin, H. Liu, X. Nie, G. Feng, J. Li, T. Xin, Q. Ai, and D. Lu, Entanglement-Enhanced Quantum Metrology in Colored Noise by Quantum Zeno Effect, Physical Review Letters 129, 070502 (2022).
- [15] E. Blumenthal, C. Mor, A. A. Diringer, L. S. Martin, P. Lewalle, D. Burgarth, K. B. Whaley, and S. Hacohen-Gourgy, Demonstration of universal control between non-interacting qubits using the Quantum of the Control of the Co

- tum Zeno effect (2021), arXiv:2108.08549 [quant-ph].
- [16] I. C. Nodurft, H. C. Shaw, R. T. Glasser, B. T. Kirby, and T. A. Searles, Generation of polarization entanglement via the quantum Zeno effect (2022), arXiv:2205.02315 [quant-ph].
- [17] N. V. Leppenen and D. S. Smirnov, Optical measurement of electron spins in quantum dots: Quantum Zeno effects (2022), arXiv:2202.13994 [cond-mat, physics:quant-ph].
- [18] S. Patsch, S. Maniscalco, and C. P. Koch, Simulation of open-quantum-system dynamics using the quantum Zeno effect, Physical Review Research 2, 023133 (2020).
- [19] P. Bethke, R. P. G. McNeil, J. Ritzmann, T. Botzem, A. Ludwig, A. D. Wieck, and H. Bluhm, Measurement of Backaction from Electron Spins in a Gate-Defined GaAs Double Quantum dot Coupled to a Mesoscopic Nuclear Spin Bath, Physical Review Letters 125, 047701 (2020).
- [20] M. T. Madzik, T. D. Ladd, F. E. Hudson, K. M. Itoh, A. M. Jakob, B. C. Johnson, J. C. McCallum, D. N. Jamieson, A. S. Dzurak, A. Laucht, and A. Morello, Controllable freezing of the nuclear spin bath in a single-atom spin qubit, Science Advances 6, eaba3442 (2020).
- [21] T. Norsen, Foundations of Quantum Mechanics: An Exploration of the Physical Meaning of Quantum Theory (Springer, Cham, Switzerland, 2017).
- [22] K. Jacobs, Quantum Measurement Theory and Its Applications (Cambridge University Press, Cambridge, 2014).
- [23] H. M. Wiseman, Quantum trajectories and quantum measurement theory, Quantum and Semiclassical Optics: Journal of the European Optical Society Part B 8, 205 (1996).
- [24] I. de Vega and D. Alonso, Dynamics of non-Markovian open quantum systems, Reviews of Modern Physics 89, 015001 (2017).
- [25] Y. Tanimura, Real-time and imaginary-time quantum hierarchal Fokker-Planck equations, The Journal of Chemical Physics 142, 144110 (2015).
- [26] J. T. Stockburger, Simulating spin-boson dynamics with stochastic Liouville-von Neumann equations, Chemical Physics The Spin-Boson Problem: From Electron Transfer to Quantum Computing ... to the 60th Birthday of Professor Ulrich Weiss, 296, 159 (2004).
- [27] G. Lindblad, On the generators of quantum dynamical semigroups, Communications in Mathematical Physics 48, 119 (1976).
- [28] K. Snizhko, P. Kumar, and A. Romito, Quantum Zeno effect appears in stages, Physical Review Research 2, 033512 (2020).
- [29] I. Percival, Quantum State Diffusion (Cambridge University Press, Cambridge, 1998).
- [30] B. J. Hiley, R. E. Callaghan, and O. Maroney, Quantum trajectories, real, surreal or an approximation to a deeper process? (2000), arXiv:quant-ph/0010020.
- [31] H. J. Carmichael, Quantum trajectory theory for cas-

- caded open systems, Physical Review Letters **70**, 2273 (1993).
- [32] N. Bohr, On the Notions of Causality and Complementarity, Science 111, 51 (1950).
- [33] E. Schrödinger, Are There Quantum Jumps? Part I, The British Journal for the Philosophy of Science 3, 109 (1952).
- [34] P. Holland, What's wrong with Einstein's 1927 hidden-variable interpretation of quantum mechanics?, Foundations of Physics 35, 177 (2005), arXiv:quant-ph/0401017.
- [35] D. Bohm, A Suggested Interpretation of the Quantum Theory in Terms of "Hidden" Variables. I, Physical Review 85, 166 (1952).
- [36] P. R. Holland, New Trajectory Interpretation of Quantum Mechanics, Foundations of Physics 28, 881 (1998).
- [37] F. Avanzini, B. Fresch, and G. J. Moro, Pilotwave quantum theory with a single Bohm's trajectory, Foundations of Physics 46, 575 (2016), arXiv:1503.00581 [quant-ph].
- [38] B. J. Hiley, M. A. de Gosson, and G. Dennis, Quantum Trajectories: Dirac, Moyal and Bohm, Quanta 8, 11 (2019).
- [39] K. W. Murch, S. J. Weber, C. Macklin, and I. Siddiqi, Observing single quantum trajectories of a superconducting quantum bit, Nature 502, 211 (2013).
- [40] A. N. Jordan, Watching the wavefunction collapse, Nature 502, 177 (2013).
- [41] M. Bellini, H. Kwon, N. Biagi, S. Francesconi, A. Zavatta, and M. S. Kim, Demonstrating quantum microscopic reversibility using coherent states of light (2022), arXiv:2205.13089 [quant-ph].
- [42] J. A. Gross, B. Q. Baragiola, T. M. Stace, and J. Combes, Master equations and quantum trajectories for squeezed wave packets, Physical Review A 105, 023721 (2022).
- [43] W. L. Power and P. L. Knight, Stochastic simulations of the quantum Zeno effect, Physical Review A 53, 1052 (1996).
- [44] M. Naghiloo, J. J. Alonso, A. Romito, E. Lutz, and K. W. Murch, Information Gain and Loss for a Quantum Maxwell's Demon, Physical Review Letters 121, 030604 (2018).
- [45] F. Helmer, M. Mariantoni, E. Solano, and F. Marquardt, Quantum nondemolition photon detection in circuit QED and the quantum Zeno effect, Physical Review A 79, 052115 (2009).
- [46] J. Gambetta, A. Blais, M. Boissonneault, A. A. Houck, D. I. Schuster, and S. M. Girvin, Quantum trajectory approach to circuit QED: Quantum jumps and the Zeno effect, Physical Review A 77, 012112 (2008).
- [47] J. Gambetta and H. M. Wiseman, Interpretation of non-Markovian stochastic Schrödinger equations as a hidden-variable theory, Physical Review A 68, 062104 (2003).
- [48] B. Skinner, J. Ruhman, and A. Nahum, Measurement-Induced Phase Transitions in the Dynamics of Entanglement, Physical Review X 9, 031009 (2019).
- [49] G. de Lange, D. Ristè, M. J. Tiggelman, C. Eichler, L. Tornberg, G. Johansson, A. Wallraff, R. N. Schouten, and L. DiCarlo, Reversing Quantum Trajectories with Analog Feedback, Physical Review Letters 112, 080501 (2014).
- [50] N. Roch, M. E. Schwartz, F. Motzoi, C. Macklin, R. Vijay, A. W. Eddins, A. N. Korotkov, K. B. Whaley, M. Sarovar, and I. Siddiqi, Observation

- of Measurement-Induced Entanglement and Quantum Trajectories of Remote Superconducting Qubits, Physical Review Letters **112**, 170501 (2014).
- [51] C. Sayrin, I. Dotsenko, X. Zhou, B. Peaudecerf, T. Rybarczyk, S. Gleyzes, P. Rouchon, M. Mirrahimi, H. Amini, M. Brune, J.-M. Raimond, and S. Haroche, Real-time quantum feedback prepares and stabilizes photon number states, Nature 477, 73 (2011).
- [52] H.-P. Breuer and F. Petruccione, The Theory of Open Quantum Systems (Oxford University Press, Oxford, 2007)
- [53] D. Matos, L. Kantorovich, and I. J. Ford, Stochastic entropy production for continuous measurements of an open quantum system (2022), arXiv:2205.07288 [cond-mat, physics:quant-ph].
- [54] K. Itô, Stochastic integral, Proceedings of the Imperial Academy 20, 519 (1944).
- [55] D. Aerts and M. Sassoli de Bianchi, The extended Bloch representation of quantum mechanics and the hidden-measurement solution to the measurement problem, Annals of Physics **351**, 975 (2014).
- [56] I. Lukach and Y. Smorodinskij, On algebra of Gell-Mann's matrices for SU(3) group, Yadernaya Fizika 27, 1694 (1978).
- [57] P. E. Kloeden and E. Platen, Stochastic Differential Equations, in Numerical Solution of Stochastic Differential Equations, Applications of Mathematics, edited by P. E. Kloeden and E. Platen (Springer, Berlin, Heidelberg, 1992) pp. 103–160.
- [58] https://drive.google.com/file/d/
 1xcBIlHtQ-pseZNxMxSvL-PG60BxXxLNH/view?
 usp=sharing (), Movie of spin 1 dynamics with
 measurement strength 3.
- [59] https://drive.google.com/file/d/
 1sNncxc19eDs8ZXe5Pt66LE_fIHOM1T_v/view?usp=
 sharing (), Movie of spin 3/2 dynamics with
 measurement strength 1.
- [60] N. Bohr, A. P. French, and P. J. Kennedy, Niels Bohr: A Centenary Volume (Harvard University Press, Cambridge, MA, 1985).
- [61] Y.-H. Kim, R. Yu, S. P. Kulik, Y. H. Shih, and M. O. Scully, A Delayed Choice Quantum Eraser (1999), arXiv:quant-ph/9903047.
- [62] V. Jacques, E. Wu, F. Grosshans, F. Treussart, P. Grangier, A. Aspect, and J.-F. Roch, Experimental Realization of Wheeler's Delayed-Choice Gedanken Experiment, Science 315, 966 (2007).
- [63] S. P. Walborn, M. O. T. Cunha, S. Padua, and C. H. Monken, A double-slit quantum eraser, Physical Review A 65, 033818 (2002), arXiv:quant-ph/0106078.
- [64] J. von Neumann, Mathematical Foundations of Quantum Mechanics (Princeton University Press, Princeton, NJ, 1955).
- [65] N. P. Oxtoby, J. Gambetta, and H. M. Wiseman, Model for monitoring of a charge qubit using a radiofrequency quantum point contact including experimental imperfections, Physical Review B 77, 125304 (2008), arXiv:0706.3527 [cond-mat, physics:quantph].
- [66] N. P. Oxtoby, P. Warszawski, H. M. Wiseman, H.-B. Sun, and R. E. S. Polkinghorne, Quantum trajectories for the realistic measurement of a solid-state charge qubit, Physical Review B 71, 165317 (2005).

Appendix A: Gell-Mann matrices

The Gell-Mann matrices used to form the spin 1 density matrix in Eq. (23) are:

$$\lambda_{1} = \begin{pmatrix} 0 & 1 & 0 \\ 1 & 0 & 0 \\ 0 & 0 & 0 \end{pmatrix} \lambda_{2} = \begin{pmatrix} 0 & -i & 0 \\ i & 0 & 0 \\ 0 & 0 & 0 \end{pmatrix} \lambda_{3} = \begin{pmatrix} 1 & 0 & 0 \\ 0 & -1 & 0 \\ 0 & 0 & 0 \end{pmatrix}$$

$$\lambda_{4} = \begin{pmatrix} 0 & 0 & 1 \\ 0 & 0 & 0 \\ 1 & 0 & 0 \end{pmatrix} \lambda_{5} = \begin{pmatrix} 0 & 0 & -i \\ 0 & 0 & 0 \\ i & 0 & 0 \end{pmatrix} \lambda_{6} = \begin{pmatrix} 0 & 0 & 0 \\ 0 & 0 & 1 \\ 0 & 1 & 0 \end{pmatrix}$$

$$\lambda_{7} = \begin{pmatrix} 0 & 0 & 0 \\ 0 & 0 & -i \\ 0 & i & 0 \end{pmatrix} \lambda_{8} = \frac{1}{\sqrt{3}} \begin{pmatrix} 1 & 0 & 0 \\ 0 & 1 & 0 \\ 0 & 0 & -2 \end{pmatrix}. \tag{A1}$$

Appendix B: Spin 1 SDEs

Itô processes for the variables parametrising the spin 1 density matrix are as follows:

$$ds = \epsilon \frac{k}{\sqrt{2}} dt - \alpha^2 \frac{s}{2} dt - \alpha \frac{s}{3} (-3 + 2\sqrt{3}u + 6z) dW$$

$$dm = -\epsilon \frac{2u + v}{\sqrt{2}} dt - \alpha^2 \frac{m}{2} dt - \alpha \frac{m}{3} (-3 + 2\sqrt{3}u + 6z) dW$$

$$du = \epsilon \frac{2m - y}{\sqrt{2}} dt + \alpha \frac{1}{\sqrt{3}} (1 - 2u^2 + \sqrt{3}u(1 - 2z) + z) dW$$

$$dv = \epsilon \frac{m - y}{\sqrt{2}} dt - 2\alpha^2 v dt - \frac{2}{3} \alpha v(\sqrt{3}u + 3z) dW$$

$$dk = \epsilon \frac{-s + x}{\sqrt{2}} dt - 2\alpha^2 k dt - \frac{2}{3} \alpha k(\sqrt{3}u + 3z) dW$$

$$dx = -\epsilon \frac{k}{\sqrt{2}} dt - \frac{1}{2} \alpha^2 x dt - \frac{1}{3} \alpha x(3 + 2\sqrt{3}u + 6z) dW$$

$$dy = \epsilon \frac{u + v - \sqrt{3}z}{\sqrt{2}} dt - \frac{1}{2} \alpha^2 y dt - \frac{1}{3} \alpha y(3 + 2\sqrt{3}u + 6z) dW$$

$$dz = \epsilon \sqrt{\frac{3}{2}} y dt - \frac{1}{3} \alpha (-1 + 2z)(3 + \sqrt{3}u + 3z) dW.$$
(B1)

Appendix C: Spin 3/2 generators

The SU(2) \otimes SU(2) generators used to form the spin 3/2 density matrix in Eq. (26) are as follows: $\Sigma_1 = I_2 \otimes \sigma_x$, $\Sigma_2 = I_2 \otimes \sigma_y$, $\Sigma_3 = I_2 \otimes \sigma_z$, $\Sigma_4 = \sigma_x \otimes I_2$, $\Sigma_5 = \sigma_x \otimes \sigma_x$, $\Sigma_6 = \sigma_x \otimes \sigma_y$, $\Sigma_7 = \sigma_x \otimes \sigma_z$, $\Sigma_8 = \sigma_y \otimes I_2$, $\Sigma_9 = \sigma_y \otimes \sigma_x$, $\Sigma_{10} = \sigma_y \otimes \sigma_y$, $\Sigma_{11} = \sigma_y \otimes \sigma_z$, $\Sigma_{12} = \sigma_z \otimes I_2$, $\Sigma_{13} = \sigma_z \otimes \sigma_x$, $\Sigma_{14} = \sigma_z \otimes \sigma_y$ and $\Sigma_{15} = \sigma_z \otimes \sigma_z$. Explicitly:

$$\Sigma_{1} = \begin{pmatrix} 0 & 1 & 0 & 0 \\ 1 & 0 & 0 & 0 \\ 0 & 0 & 0 & 1 \\ 0 & 0 & 1 & 0 \end{pmatrix} \Sigma_{2} = \begin{pmatrix} 0 & -i & 0 & 0 \\ i & 0 & 0 & 0 \\ 0 & 0 & 0 & -i \\ 0 & 0 & i & 0 \end{pmatrix} \\
\Sigma_{3} = \begin{pmatrix} 1 & 0 & 0 & 0 \\ 0 & -1 & 0 & 0 \\ 0 & 0 & 1 & 0 \\ 0 & 0 & 0 & -1 \end{pmatrix} \Sigma_{4} = \begin{pmatrix} 0 & 0 & 1 & 0 \\ 0 & 0 & 0 & 1 \\ 1 & 0 & 0 & 0 \\ 0 & 1 & 0 & 0 \\ 1 & 0 & 0 & 0 \end{pmatrix} \\
\Sigma_{5} = \begin{pmatrix} 0 & 0 & 1 \\ 0 & 1 & 0 \\ 0 & 1 & 0 & 0 \\ 1 & 0 & 0 & 0 \end{pmatrix} \Sigma_{6} = \begin{pmatrix} 0 & 0 & 0 & -i \\ 0 & 0 & i & 0 \\ 0 & -i & 0 & 0 \\ 0 & i & 0 & 0 \end{pmatrix} \\
\Sigma_{7} = \begin{pmatrix} 0 & 0 & 1 & 0 \\ 0 & 0 & 0 & -1 \\ 1 & 0 & 0 & 0 \\ 0 & -1 & 0 & 0 \end{pmatrix} \Sigma_{8} = \begin{pmatrix} 0 & 0 & -i & 0 \\ 0 & 0 & 0 & -i \\ i & 0 & 0 & 0 \\ 0 & i & 0 & 0 \end{pmatrix} \\
\Sigma_{9} = \begin{pmatrix} 0 & 0 & -i & 0 \\ 0 & 0 & -i & 0 \\ 0 & i & 0 & 0 \\ i & 0 & 0 & 0 \end{pmatrix} \Sigma_{10} = \begin{pmatrix} 0 & 0 & 0 & -1 \\ 0 & 0 & 1 & 0 \\ 0 & -1 & 0 & 0 \\ 1 & 0 & 0 & 0 \\ 0 & 0 & -1 & 0 \\ 0 & 0 & 0 & -1 \end{pmatrix} \\
\Sigma_{13} = \begin{pmatrix} 0 & 1 & 0 & 0 \\ 1 & 0 & 0 & 0 \\ 0 & 0 & -1 & 0 \\ 0 & 0 & -1 & 0 \end{pmatrix} \Sigma_{14} = \begin{pmatrix} 0 & -i & 0 & 0 \\ i & 0 & 0 & 0 \\ 0 & 0 & 0 & i \\ 0 & 0 & -i & 0 \end{pmatrix} \\
\Sigma_{15} = \begin{pmatrix} 1 & 0 & 0 & 0 \\ 0 & -1 & 0 & 0 \\ 0 & 0 & -1 & 0 \\ 0 & 0 & 0 & 1 \end{pmatrix}. \quad (C1)$$

Appendix D: Spin 3/2 SDEs

Itô processes for the variables parametrising the spin 3/2 density matrix are as follows:

$$dv = -\epsilon o dt - \frac{1}{2}\alpha^2 v dt + \alpha(2q - v(f + 2p)) dW$$

$$de = \epsilon(\sqrt{3}f + k) dt - \frac{1}{2}\alpha^2 e dt + \alpha(2s - e(f + 2p)) dW$$

$$df = -\epsilon(\sqrt{3}e + j - m) dt - \alpha(-1 + f^2 + 2fp - 2u) dW$$

$$dg = -\epsilon s dt - 2\alpha^2 g dt + \alpha(k - g(f + 2p)) dW$$

$$dh = -\frac{1}{2}\alpha^2(5h - 4n) dt - \alpha h(f + 2p) dW$$

$$dj = \epsilon(f + \sqrt{3}k - p) dt - \frac{1}{2}\alpha^2(5j + 4m) dt - \alpha j(f + 2p) dW$$

$$dk = -\epsilon(e + \sqrt{3}j) dt - 2\alpha^2 k dt + \alpha(g - k(f + 2p)) dW$$

$$dl = \epsilon q dt - 2\alpha^2 l dt + \alpha(o - l(f + 2p)) dW$$

$$dm = \epsilon(-f + p) dt - \frac{1}{2}\alpha^2(4j + 5m) dt - \alpha m(f + 2p) dW$$

$$dn = \epsilon \sqrt{3}o dt + \alpha^2(2h - \frac{5n}{2}) dt - \alpha n(f + 2p) dW$$

$$do = \epsilon(-\sqrt{3}n + v) dt - 2\alpha^2 o dt + \alpha(l - o(f + 2p)) dW$$

$$dp = \epsilon(j - m) dt + \alpha(2 - p(f + 2p) + u) dW$$

$$dq = -\epsilon l dt - \frac{1}{2}\alpha^2 q dt - \alpha(fq + 2pq - 2v) dW$$

$$ds = \epsilon(g + \sqrt{3}u) dt - \frac{1}{2}\alpha^2 s dt + \alpha(2e - s(f + 2p)) dW$$

$$du = -\epsilon \sqrt{3}s dt + \alpha(2f + p - u(f + 2p)) dW.$$
(D1)